Theory of Zener tunneling and Wannier-Stark states in semiconductors

Aldo Di Carlo and P. Vogl
Walter Schottky Institut and Physics Department, Technische Universität München, 85748 Garching, Federal Republic of Germany

W. Pötz
Department of Physics, University of Illinois, Chicago, Illinois 60680
(Received 17 May 1994)

A general multiband and multichannel scattering theory of the current in mesoscopic-device structures is developed and applied to the Zener diode. It takes into account the realistic electronic structure, its modification by the high electric field, and the field-free contact regions in a nonperturbative manner. This theory elucidates the interplay between Zener tunneling and Wannier-Stark resonances. Quantitative conditions for the occurrence of Wannier-Stark oscillations in the current of a bulk semiconductor or superlattice are derived. It is predicted that Wannier-Stark resonances are detectable in the interband tunneling current of highly doped submicrometer p-i-n diodes with very short i zones. We show that there are two regimes in the Zener tunneling current: a low-field or Zener regime where the conductance is a smooth function of the applied voltage, and a high-field or Stark regime where Wannier-Stark resonances are induced.

I. INTRODUCTION

Since Zener (1934) explained the electric breakdown mechanism in solids in terms of band-to-band tunneling, the phenomenon of Zener tunneling has attracted much interest, particularly since it is relevant in modern nanoscale devices. In spite of much progress in the understanding of interband tunneling (see, e.g., Refs. 1 and 2), the existence of Wannier-Stark (WS) localization and the relation between Zener tunneling and Stark ladders is still controversial.[3–6]

In this paper, we present a general theory for the interband tunneling current in semiconductors that takes into account the electronic structure and the nonuniformity of the electric field in a device in a realistic fashion. We provide quantitative criteria for the existence of WS resonances in the Zener current and predict that one can observe these resonances in bulk transport experiments. By developing a multiband multichannel scattering theory for interband tunneling that consistently includes the asymptotic contact regimes in a device, we can resolve some of the long-standing controversies about the relation between Zener tunneling and WS ladders.

The concept of Stark ladders was introduced by Wannier[7] who analyzed the spectrum of a crystal Hamiltonian H_F in the presence of a uniform electric field. In a one-band approximation, Wannier found its eigenvalues E_ν to consist of discrete, equidistant levels with square integrable wave functions,

$$E_\nu = \langle \varepsilon'_{\mathbf{k}} \rangle + \nu \frac{2\pi e|\mathbf{F}|}{|\mathbf{G}|}. \tag{1}$$

Here, $\mathbf{F}$ is the electric field, $\mathbf{G}$ is the shortest reciprocal lattice vector in the direction of the field, $\varepsilon'_{\mathbf{k}}$ is related to the zero-field Bloch eigenvalues and the average is performed over all wave vectors in the Brillouin zone parallel to $\mathbf{F}$. Throughout this paper, e denotes the magnitude of the electronic charge.

This work stimulated a long controversy about the existence of these so-called WS ladders in the spectrum of the full many-band Hamiltonian H_F.[3–10] Indeed, the energy spectrum of H_F was shown to be continuous and does *not* contain localized states.[11] Only recently, a rigorous mathematical theory was developed for one-dimensional systems that showed that H_F does not possess eigenvalues of the form of Eq. (1).[11] However, there do exist equidistant Stark *resonances* of finite width, provided the spectrum of the field-free Hamiltonian possesses energy gaps and the width of the energy bands is finite.[10–14]

Up to now, however, these rigorous results have not been extended to realistic three-dimensional semiconductors and to nonuniform fields. In fact, many of the controversies about WS ladders originate in the commonly used assumption of an infinitely extended, uniform electric field. This uniform field approximation leads to several inconsistencies and artifacts. First, a periodic solid in a uniform electric field does not possess propagating bulklike scattering states that are a prerequisite for calculating a well-defined current in a finite potential drop. Second, a system in an infinitely extended constant electric field has no ground state. Third, within the uniform field approximation, the energy spectrum of H_F is a chaotic function of the field direction, since the slightest change in the field direction alters the periodicity of the Hamiltonian along the field direction.[15]

Experimentally, there have been several attempts to identify WS resonances in bulk semiconductors.[16–19] No clear evidence has been found so far. However, our calculations show that the formation of WS resonances, as

well as their signature in the tunneling current, require extremely high built-in electric fields. Such structures are becoming achievable only due to recent progress in molecular-beam epitaxy. This is in contrast to the situation in superlattices, where WS resonances have been clearly resolved, albeit, in optical experiments.[20–22]

Next to WS ladders, another quantity of fundamental interest in connection with high electric fields is the interband or Zener tunneling current that can be observed in devices with high reverse bias. The Zener current has been calculated in two classic papers by Kane.[23,24] Kane also employed the uniform field approximation and expanded the wave function of the three-dimensional H_F in terms of Bloch functions.[25] He obtained the equation

$$\left[\varepsilon_n(\mathbf{k}) - ieF\frac{\partial}{\partial k_z} - eFX_{nn} - E\right] a_n(\mathbf{k}) - eF\sum_{m\neq n} X_{nm}a_m(\mathbf{k}) = 0, \quad (2)$$

where

$$X_{nm}(\mathbf{k}) = i\int u^*_{n\mathbf{k}}\frac{\partial}{\partial k_z}u_{m\mathbf{k}}d\mathbf{r}, \quad (3)$$

denotes the interband matrix element containing the periodic part of the Bloch functions $u_{n\mathbf{k}}$. In Eq. (2), $\varepsilon_n(\mathbf{k})$ is the band structure for zero field and the $a_n(\mathbf{k})$ represent the expansion coefficients of the wave function. By treating the interband terms in Eq. (2) in first-order perturbation theory, and by evaluating $\varepsilon_n(\mathbf{k})$ in terms of a two-band $\mathbf{k}\cdot\mathbf{p}$ model, Kane obtained a WKB-like expression for the transmission coefficient,[23,24,26–28]

$$T(F,k_\parallel) = \frac{\pi^2}{9}e^{-\frac{E_g}{2E_F}}e^{-\frac{2E_\parallel}{E_F}} + S(F), \quad (4)$$

with

$$E_\parallel = \hbar^2\mathbf{k}_\parallel^2/2m^*,$$

$$E_F = \sqrt{2}\hbar eF/\pi\sqrt{m^*E_g}.$$

Here, E_g is the energy gap and $\mathbf{k}_\parallel$ the planar momentum perpendicular to the field direction. The mass parameter m^* is a function of the valence and conduction band masses, $2/m^* = 1/m_c + 1/m_v$. The last term $S(F)$ in this equation was neglected by Kane and yields a small oscillatory term in the field.[26,28]

It has been pointed out by Argyres and Sfiat,[29] that the theory of Zener tunneling, as sketched above, contains several assumptions that become invalid for high fields. For very high fields, the interband elements in Eq. (2) cannot be treated as a small perturbation. In addition, a $\mathbf{k}\cdot\mathbf{p}$ two-band model does not lead to a finite band width and, therefore, never supports WS resonances, no matter how high the field is (see Sec. III C). Finally, interband tunneling in a bulk semiconductor requires a very high electric field which can only be reached in an extremely thin sheet of the active device region. This is in conflict with the uniform field approximation that has been employed almost exclusively in studies of high-field properties of solids.[1,2,29]

Our paper is organized as follows. In Sec. II, we develop an elastic multichannel scattering theory for the current response in mesoscopic solid-state device structures which is applicable under very general boundary conditions, such as an arbitrary number of contact regions of different spatial dimensions and electronic structure. This task involves the construction of a suitable steady-state density operator, correct normalization and a general proof of orthogonality of scattering states for nonvanishing potential asymptotics, derivation of a general expression for the current density in response to a (finite) applied bias within an effective independent-particle picture and, finally, application to the Zener diode. The technical details of the key issues in this derivation and a discussion of validity is presented in the Appendices A-D. In Sec. III, numerical results and concrete predictions of the Zener tunneling rate and the appearance of WS states in the interband current are presented. In Sec. IV, we critically examine and summarize the prerequisites for detecting WS states in transport experiments.

II. MULTICHANNEL SCATTERING THEORY

In this section, we develop a consistent theoretical formulation of the current-voltage characteristics of mesoscopic device structures within the framework of elastic scattering theory. It forms the basis for the subsequent treatment of the Zener diode. In particular, we will show that the Zener current [Eq. (12)] is determined by a Landauer-Büttiker-type expression[30,31] which is applicable to multiband and multichannel situations with an arbitrary number of different contact regimes, very high electric fields and, consequently, nontrivial potential asymptotics.

Application of time-dependent scattering theory allows a general proof of orthogonality of scattering states in mesoscopic device structures, an issue which has been under debate in the past.[32–34] This is a central issue for the calculation of absolute current densities. A theory of the Zener diode must be based on a realistic many-band treatment and, therefore, calls for the development of a time-dependent scattering theory where, asymptotically, the particles are not free (effective-mass-like), but move in the periodic potential of a crystal.[35] As a by-product, this approach provides a straightforward proof of equivalence between conductance formulas (i.e., a conductance proportional to transmission coefficients) and linear-response theory for an open system. This issue, as well as the proper procedure to derive such a result, has been under some discussion in the recent past.[36] Finally, the conditions under which the linear-response result is valid for *finite* applied bias are discussed.

A. Mesoscopic multichannel devices

We consider a general electronic device to consist of (i) a device region, (ii) connecting leads or transition

regions, and (iii) an arbitrary number of particle reservoirs. Here, the device may be any structure which exploits the wave nature of electrons and provides predominantly elastic propagation of charge carriers, such as electronic wave guides, (resonant) tunneling structures, constrictions, etc. The leads generally are transition regions which mediate particle exchange between the device and reservoirs. Each of the reservoirs R is characterized dynamically by a reservoir Hamiltonian $H_{o,R}$ and macroscopically by a set of thermodynamic parameters, such as temperature and chemical potentials. For a solid-state electronic device, reservoirs will usually be crystals of some given spatial dimension. A simple situation with two-particle reservoirs and a single device region is depicted in Fig. 1. Associated with each reservoir are a number of "in" and "out" channels characterized by $(R, n, k^{\mp})$, in the sense of quantum scattering theory, where "−" refers to "in," i.e., towards the device, and "+" to "out," i.e., away from the device (see Fig. 1).[37] n denotes a set of discrete quantum numbers, such as spin, band and/or subband indices. k denotes a set of quantum numbers which, in the thermodynamic limit, become continuous, such as the D_R components of Bloch vectors. For simplicity, the vector nature of Bloch vectors $\mathbf{k}$ will generally be suppressed in the notation of this section.

Except for the leads and regardless of any bias applied across the device, individual reservoirs are assumed to be isolated from each other and to be "infinitely" large in the sense that, sufficiently deep inside the reservoirs, thermal equilibrium is maintained. This condition is imperative to allow a clear definition of the applied bias within an elastic scattering approach. It implies that the current density and net charge density vanish sufficiently deep inside the reservoirs. For systems with a unidirectional field, such as the Zener diode, in the steady state the current density must be small *throughout* the structure, such that the carrier distribution deep in the reservoirs remains undisturbed. Therefore, one either is confined to linear response or one must attach higher-dimensional reservoirs to guarantee that the transmission probability between these reservoirs is (infinitesimally) small.

Before proceeding with the theoretical part it is useful to explain the notation which will be used throughout this paper. H_o denotes the effective one-particle Hamiltonian of the system (device plus reservoirs) in thermal equilibrium. Its eigenstates $|\nu\rangle$ may be bound states $|b\rangle$ and scattering states $|\psi^{+}_{R,n,k}\rangle$. Its channel Hamiltonians are $H_{o,R} = \lim_{\mathbf{x}\to R} H_o$, where $\lim_{\mathbf{x}\to R}$ denotes $\mathbf{x}$ going to infinity inside of reservoir R. The channel Hamiltonians have eigenstates $|\phi_{R,n,k}\rangle$ which serve as channel states (in or out asymptotes) of the scattering states of H_o and H. $H = H_o + U$ denotes the effective one-particle Hamiltonian in the steady state of the system under applied bias. Its eigenstates $|N\rangle$ may be bound states $|B\rangle$ and scattering states $|\Psi^{+}_{R,n,k}\rangle$. Its channel Hamiltonians are $H_R = H_o + U_R(\infty)$, where $U_R(\infty) = \lim_{\mathbf{x}\to R} U(\mathbf{x})$. The decay

$$|U(\mathbf{x}) - U_R(\infty)| \to 0 \quad \text{for } \mathbf{x} \to R, \tag{5}$$

must occur sufficiently fast to allow formulation of scattering theory. No universal criteria exist; however, special cases have been studied in the literature. See, for example, Refs. 37, 35, and 38. Under condition (5) the continuous spectrum $\sigma^{(H)}_{ac}$ of H is determined by the continuous spectra $\sigma^{(R)}_{ac}$ of the channel Hamiltonians H_R, $\sigma^{(H)}_{ac} = \cup_R \sigma^{(R)}_{ac}$.

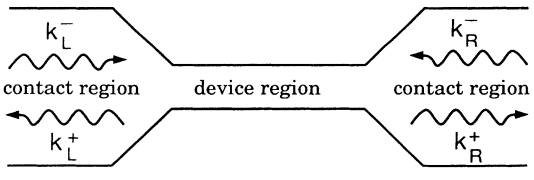

FIG. 1. Schematic picture of a tunneling diode consisting of a device region in the center and two adjacent semibulk particle reservoirs. The in-channel states of each reservoir denote states propagating towards the device and are labeled with "−". The out- or "+" channel states propagate away from the device region.

B. The steady-state density operator

The steady-state density operator $\rho(0)$ used to calculate the current response is constructed using an adiabatic switching procedure applied to the equilibrium density operator,[39]

$$\rho_o = \sum_{R,n,k} f_{R,n,k} |\psi^{+}_{R,n,k}\rangle\langle\psi^{+}_{R,n,k}| + \sum_b f_b |b\rangle\langle b|. \tag{6}$$

f_ν are Fermi-Dirac distribution functions which determine occupancy of eigenstates of H_o. A general procedure to approximately reduce interacting many-body systems to effective independent-particle subsystems has been developed in Ref. 40.

Within linear response, i.e., in the limit of (infinitesimally) small applied potential, one can show that (see Appendix B)

$$\rho(0) = \sum_{R,n,k} f_{R,n,k} |\Psi^{+}_{R,n,k}\rangle\langle\Psi^{+}_{R,n,k}| + \sum_b f_b |B\rangle\langle B|. \tag{7}$$

One observes that the occupation probability of bound states $|B\rangle$ of H are those of the corresponding, via first-order perturbation theory, bound states $|b\rangle$ of H_o. Scattering states $|\Psi^{+}_{R,n,k}\rangle$ of H have the same occupation probability in $\rho(0)$ as scattering states $|\psi^{+}_{R,n,k}\rangle$ of H_o with the *same in asymptote* (R, n, k) in ρ_o.

Considering structures without bound states, the above expression is also valid for *finite* applied bias if the transmission coefficients between the reservoirs are infinitesimally small. The latter, however, was a necessary condition from the beginning for keeping reservoirs in thermal equilibrium when a finite bias is applied across the device. A more detailed discussion of this critical issue is given in Appendix B.

In Appendices B–D we show that traditional scattering theory is fully applicable to the type of many-channel

device systems as envisioned here. The presence of nontrivial potential asymptotics, such as nonzero or periodic potential asymptotics, provide no conceptual complications. In particular, we identify proper normalization of the scattering states $|\Psi^+_{R,n,k}\rangle$ and show that they are, under very general conditions, orthogonal in a generalized sense of improper eigenfunctions. Consequently, a unitary S matrix may be defined, as detailed in Appendix D.

C. Average reservoir current densities

The steady-state current density in any given reservoir may be calculated from the expectation value of the velocity operator

$$\mathbf{v} = \langle \mathbf{V} \rangle = \frac{i}{\hbar} \langle [H, \mathbf{X}] \rangle .$$

Here, $\mathbf{X}$ and $\mathbf{V}$ denote position and velocity operator, respectively. $\langle \cdots \rangle$ denotes the statistical average with respect to $\rho(0)$. Individual stationary scattering states must fulfill Kirchhoff's junction rule and their contribution to the current in reservoir R is expressed most conveniently using their asymptotic time evolution,

$$|\Psi^+_{R,n,k}(t)\rangle|_{t\to-\infty} \to |\phi_{R,n,k^-}(t)\rangle, \tag{8}$$

and

$$|\Psi^+_{R,n,k}(t)\rangle|_{t\to+\infty} \to \sum_{\bar{R},\bar{n}} \int_{E_{R,n}(k)} d\mathcal{S}_{\bar{R},\bar{n}} \times b_{(R,n,k^-\to\bar{R},\bar{n},\bar{k}^+)} |\phi_{\bar{R},\bar{n},\bar{k}^+}(t)\rangle, \tag{9}$$

with

$$\int_{\mathrm{BZ},\bar{n}} d^{(D_R)}\bar{k}^{\pm} = \int dE \int_E \frac{d\mathcal{S}_{\bar{R},\bar{n}}}{|\nabla_{\bar{k}} E_{\bar{R},\bar{n}}(\bar{k})|} ,$$

for given energy band $\bar{n}$. These formal limits hold when scattering states are used as basis functions for wave packets with incidence through reservoir R for $t \to -\infty$ and exit through any reservoir $\bar{R}$ for $t \to +\infty$, in the usual sense of scattering theory. Here, we consider a situation where Bloch states form the asymptotic channel states. The $\bar{k}$ integral is over the energy surface $\mathcal{S}$ of "out" states $(\bar{R},\bar{n},\bar{k}^+)$ of energy $E = E_{R,n}(k) = E_{\bar{R},\bar{n}}(\bar{k})$. Note that time-reversal symmetry causes that the energy surface for "in" channels equals that for "out" channels. The relation between "in" and "out" channel states *normalized to unit velocity* may be expressed in form of a unitary S matrix, Appendix D,

$$\begin{aligned} S_{(\bar{R},\bar{n},\bar{k}^+),(R,n,k^-)} &= b_{(R,n,k^-\to\bar{R},\bar{n},\bar{k}^+)} \sqrt{\frac{v_{\bar{R},\bar{n},\bar{k}}}{v_{R,n,k}}} \\ &= \delta_{R,\bar{R}}\delta_{n,\bar{n}}\delta_{k,\bar{k}} r_{(R,n,k^-\to R,n,k^+)} \\ &\quad + (1-\delta_{R,\bar{R}}\delta_{n,\bar{n}}\delta_{k,\bar{k}}) t_{(R,n,k^-\to\bar{R},\bar{n},\bar{k}^+)}, \end{aligned} \tag{10}$$

defining transmission and reflection amplitudes, $t_{(\mathrm{in}\to\mathrm{out})}$ and $r_{(\mathrm{in}\to\mathrm{out})}$, between channels $(R,n,k^\pm)$. The velocity associated with channel state $|\phi_{R,n,k^\pm}\rangle$ is denoted by

$$\mathbf{v}_{R,n,k} = (2\pi)^{D_R} |\langle \phi_{R,n,k^\pm} | \mathbf{V} | \phi_{R,n,k^\pm} \rangle| / \Omega_R,$$

where D_R denotes the spatial dimension of reservoir R and Ω_R its normalization volume prior to the thermodynamic limit.

The average velocity of the system is

$$\langle \mathbf{V} \rangle = \frac{i}{\hbar} \sum_{R,n} \int d^{(D_R)}k f_{R,n,k^-} \langle \Psi^+_{R,n,k} | [H, \mathbf{X}] | \Psi^+_{R,n,k} \rangle .$$

The total current density deep in reservoir R (deep enough to allow the use of the asymptotic form of scattering states) arises from influx through reservoir R,

$$\sum_n \int d^{(D_R)}k^- f_R(E_{R,n}(k)) (-\mathbf{v}_{R,n,k^+}) \frac{(-e)}{(2\pi)^{D_R}},$$

and transmission from channels $(\bar{R},\bar{n},\bar{k}^-)$ into reservoir R,

$$\sum_{\bar{R},\bar{n}} \int d^{(D_R)}\bar{k}^- f_{\bar{R}}(E_{\bar{R},\bar{n}}(\bar{k})) \sum_n \int_{E_{\bar{R},n}(\bar{k})} d\mathcal{S}_{R,n} \times |b_{(\bar{R},\bar{n},\bar{k}^-\to R,n,k^+)}|^2 \mathbf{v}_{R,n,k^+} \frac{(-e)}{(2\pi)^{D_R}}.$$

Since the reservoirs remain in thermal equilibrium, $f_{R,n,k} = f_R(E_{R,n}(k))$. Here we have used that velocity matrix elements are diagonal in degenerate channel eigenstates.[25,38] Using unitarity of the S matrix one obtains for the average total current density in reservoir R

$$\begin{aligned} \mathbf{j}_R = \frac{(-e)}{(2\pi)^{D_R}} \sum_n \int d^{(D_R)}k \sum_{\bar{R},\bar{n}} \int_{E=E_{R,n}(k)} d\mathcal{S}_{\bar{R},\bar{n}} \\ \times [T_{(\bar{R},\bar{n},\bar{k}^-\to R,n,k^+)} f_{\bar{R}}(E) \\ - T_{(R,n,k^-\to\bar{R},\bar{n},\bar{k}^+)} f_R(E)] \\ \times \mathbf{v}_{R,n,k^+}, \end{aligned} \tag{11}$$

where $T_{(i\to j)} = |t_{(i\to j)}|^2$ denotes the transmission probability from "in" channel "i" to "out" channel "j." Note that solely transmission from $\bar{R} \neq R$ survives in (11). This is a most general expression for the current density in reservoir R within an effective independent-particle picture. It is applicable to a variety of geometries with arbitrary number, spatial dimensions and electronic structure of system and reservoirs. In case of time-reversal symmetry, one has $T_{(i\leftrightarrow j)} \equiv T_{(i\to j)} = T_{(j\to i)}$.

D. Application to the Zener diode

This approach is applied to highly-doped p-i-n junctions where the electric field due to doping and applied bias is assumed to be unidirectional, i.e., functions of z only. In this case, we have two three-dimensional reservoirs (L and R) in form of semi-infinite crystalline bulk regions which are characterized by identical Hamiltoni-

ans, except for a constant shift in energy which equals the net potential drop eV_D across the diode. Note that H_o contains the built-in potential due to doping, whereas the diode with externally applied bias corresponds to $H = H_o + U(z)$. The total z-dependent electrostatic potential which accounts for doping and the external field will be denoted by $V(z)$. For both $U(z)$ and $V(z)$ property (5) is required throughout this paper.

Utilizing that $\mathbf{k}_\parallel$, spin, and energy E are conserved in an elastic tunneling process through the Zener diode, one may simplify (11) to

$$j = \frac{(-e)}{(2\pi)^3\hbar}\int_{BZ_\parallel} d\mathbf{k}_\parallel \int_{-\infty}^{+\infty} dE \times \sum_{k_j^-}\sum_{k_i^+} T_{(L,k_j^-\to R,k_i^+)}(\mathbf{k}_\parallel, E)[f_R(E) - f_L(E)]. \quad (12)$$

Integration over $\mathbf{k}_\parallel$ is performed over the projection of the Brillouin zone onto the k_x-k_y plane. For computational purposes, scattering states, $|\Psi^+_{R,k_j}(\mathbf{k}_\parallel, E)\rangle$, are most conveniently characterized by their reservoir R, energy E, $\mathbf{k}_\parallel$, and the z component $k_j, j = z_1, z_2, \ldots$ of the real k vectors which, in the bulk regions L and R, solve $E = E_n(\mathbf{k}_\parallel, k_j)$. Here, spin is not included explicitly in the label, for brevity, even though spin-orbit effects are taken into account in the present calculations. $T_{(L,k_j^-\to R,k_i^+)}(\mathbf{k}_\parallel, E)$ denotes the transmission coefficients of the structure at given energy E and $\mathbf{k}_\parallel$.

E. Calculation of scattering states of a Zener diode

Any realistic electronic structure calculation of the scattering states $|\Psi^+_{R,k_j}(\mathbf{k}_\parallel, E)\rangle$ of p-i-n semiconductor diodes and, consequently, of the Zener current, must (i) take into account the absence of translational invariance along the field direction in the diode and (ii) treat the electric field on an equal footing with the periodic ionic potential. We use a multiband transfer matrix approach[41–43] within the framework of the empirical tight-binding method.[44,45] This allows us to investigate Zener diodes of submicrometer dimensions which contain several hundreds of atomic layers.

For computational purposes, we subdivide the diode into three regions (see Fig. 2), namely field-free highly doped contact regions L and R to the left and to the right, respectively, and an active region M where the electric field is nonzero. In regions L and R, the Hamiltonian is given by the field-free crystal Hamiltonian. We represent the latter by a first-nearest neighbor sp^3s^* tight-binding model that includes spin-orbit interaction.[44,45] The tight-binding parameters for GaAs and InSb are from Ref. 44 and Ref. 45, respectively. This Hamiltonian defines the possible in-channel states for given $\mathbf{k}_\parallel$ and E. In fact, for given $(\mathbf{k}_\parallel, E)$ the eigenfunctions of each of the two channel Hamiltonians include propagating Bloch states for which k_j corresponding to real k_z, as well as evanescent Bloch states for which k_j corresponds to complex k_z. These solutions fall into two classes. The first class

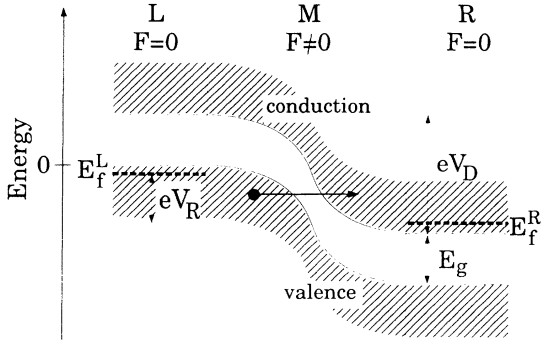

FIG. 2. Schematic picture of the tilted electronic band edge states in a typical p-n or p-i-n junction with a high electric field. The total potential drop (V_D) is defined as the potential difference between the left and right semibulk region (L, R). The reverse bias (V_r) is the difference between the Fermi levels in the L and R regions. High n and p doping ensures that the field is nonzero only in the M region. In this and all following figures, the zero of energy lies at the top of the valence band in the left (p-doped) semibulk region.

of functions, labeled $|\phi_{R,k_j^-}\rangle$, either have a group velocity $\mathbf{v}_{R,k_z}(\mathbf{k}_\parallel, E)$ pointing towards the M region if k_j is real, or, decay towards the M region if k_j is complex. Only the former provide suitable in-channel states for scattering states $|\Psi^+_{R,k_j}(\mathbf{k}_\parallel, E)\rangle$. The second class of functions, $|\phi_{R,k_j^+}\rangle$, have $\mathbf{v}_{R,k_z}(\mathbf{k}_\parallel, E)$ pointing away from the M region (out-channel states) if k_j is real, or decay towards the reservoir R if k_j is complex. With 20 localized basis functions per bulk unit cell, there are 10 solutions in each class for given $(\mathbf{k}_\parallel, E)$. There is a linear dependence between the two sets of 20 eigenfunctions associated with each of the two bulk reservoir Hamiltonians. It may be determined by matching the solutions across the central region M via a technique developed in Ref. 42.

In region M, the field is nonzero and we expand the electron wave function in terms of layered Bloch functions, using that the system is periodic in the x and y direction. The Hamiltonian matrix in this region includes, in addition to the sp^3s^* tight-binding matrix elements, the electrostatic potential $V(z)$. The latter is taken into account by adding to all on-site matrix elements the matrix element of the macroscopic potential energy $\langle w(\mathbf{X})|V(z)|w(\mathbf{X})\rangle \approx V(X_z)$.[46] Here, $|w(\mathbf{X})\rangle$ denote the linear combination of atomic orbitals (LCAO) basis states localized at the atomic position $\mathbf{X}$. We would like to stress that this does not imply that we assume the potential to be a discontinuous function of position or the basis functions to be δ functions. In any LCAO-type method, it is only the average of $V(z)$ integrated over an orbital density that enters the calculation. In principle, $V(z)$ should be calculated self-consistently from the scattering states. We have sidestepped this procedure by determining the potential according to the depletion approximation since the latter is known to be adequate for simple diode geometries, such as the one studied here.[47]

As mentioned above, the eigenstates of the reservoir

Hamiltonians H_L and H_R, respectively, may be used as basis functions in the corresponding reservoirs. Thus, for given $(\mathbf{k}_\parallel, E)$, any eigenfunction of the full Hamiltonian H, such as the scattering states $|\Psi^+_{R,k_j}(\mathbf{k}_\parallel, E)\rangle$, may, in region L, be written as

$$\langle z|\Psi^+(\mathbf{k}_\parallel, E)\rangle = \sum_i [f^-_{L,i}\langle z|\phi_{L,k_i^-}(\mathbf{k}_\parallel, E)\rangle + f^+_{L,i}\langle z|\phi_{L,k_i^+}(\mathbf{k}_\parallel, E)\rangle], \text{ for } z \text{ in } L\ . \tag{13}$$

Similarly, using the eigenfunctions of H_R for a basis,

$$\langle z|\Psi^+(\mathbf{k}_\parallel, E)\rangle = \sum_i [f^-_{R,i}\langle z|\phi_{R,k_i^-}(\mathbf{k}_\parallel, E)\rangle + f^+_{R,i}\langle z|\phi_{R,k_i^+}(\mathbf{k}_\parallel, E)\rangle], \text{ for } z \text{ in } R\ . \tag{14}$$

In order to obtain $\langle z|\Psi^+(\mathbf{k}_\parallel, E)\rangle$ in all space and to find the relation between the expansion coefficients $f^\pm_{L/R,i}$, one needs to match the solutions in regions L and R, Eqs. (13) and (14), with those in region M, which is accomplished via the transfer matrix method. The relation between the expansion coefficients $f^\pm_{L,i}$ and $f^\pm_{R,j}$ allows determination of the asymptotic form of all scattering states for given $(\mathbf{k}_\parallel, E)$ and thus the associated transmission coefficients.

Let us consider, for example, the calculation of the transmission coefficients associated with scattering state $|\Psi^+_{L,k_j^-}(\mathbf{k}_\parallel, E)\rangle$. This scattering state has an in asymptote which is an eigenstate (Bloch function) of H_L characterized by E, $\mathbf{k}_\parallel$, and real k_j^-. Thus we choose $f^-_{L,i} = \delta_{ij}$ and $f^-_{R,i} = 0$, for all i. The remaining coefficients can been shown to follow from a matrix equation of the form[42,48,49]

$$\begin{bmatrix} \mathbf{f}^+_R \\ \mathbf{f}^-_R \end{bmatrix} = \mathbf{P} \begin{bmatrix} \mathbf{f}^-_L \\ \mathbf{f}^+_L \end{bmatrix}. \tag{15}$$

The matrix $\mathbf{P}$ is the product of transfer matrices in the transition region M, multiplied by unitary matrices $\mathbf{U}$ that transform the complex Bloch functions in Eqs. (13) and (14) to the layer representation. We refer to Refs. 42, 48, 49 for the technical details. The transmission coefficient is then

$$T_{(L,k_j^-\ \to\ R,k_i^+)}(\mathbf{k}_\parallel, E) = |f^+_{R,i}|^2 \frac{|\mathbf{v}_{R,k_i^+}(\mathbf{k}_\parallel, E)|}{|\mathbf{v}_{L,k_j^-}(\mathbf{k}_\parallel, E)|}, \tag{16}$$

where, in this case, $f^+_{R,i}$ is, of course, identical to $t_{L,E,\mathbf{k}_\parallel,k_j^- \to R,E,\mathbf{k}_\parallel,k_i^+}$ in the S matrix, Eq. (10). Similarly, Eq. (15) may be solved for each incoming state from the left and from the right.

The method sketched very briefly above can also be used to calculate bound states of the electrons. The matrix $\mathbf{P}$ in Eq. (15) is composed of four submatrices,

$$\mathbf{P} = \begin{bmatrix} \mathbf{P}^{+-} & \mathbf{P}^{++} \\ \mathbf{P}^{--} & \mathbf{P}^{-+} \end{bmatrix}.$$

For a localized state, one has $\mathbf{f}^-_R = \mathbf{f}^-_L = 0$. With Eq. (15), this yields the condition $\det \mathbf{P}^{-+}(\mathbf{k}_\parallel, E) = 0$. The energies E that fulfill this equation are the localized energy eigenstates.

Once the scattering states have been determined, we can finally evaluate the current as given by Eq. (12). However, an inclusion of the complete band structure of valence and conduction bands in the calculation of the Zener current calls for integration over both energy and momentum. This is computationally very time consuming and has, to our knowledge, not been carried out previously. In situations involving only a single parabolic band, one can often simplify the transmission coefficient to the form[48] $T(\mathbf{k}_\parallel, E) \to T(\mathbf{0}, E - E_\parallel)$, where $E_\parallel = \hbar^2\mathbf{k}_\parallel^2/2m^*$. In the case of interband tunneling, however, this is not possible. Since the gap along the z direction rapidly increases with nonzero $\mathbf{k}_\parallel$, T depends exponentially on both energy E and $\mathbf{k}_\parallel$. To perform the required full $\mathbf{k}_\parallel$ integrations over the irreducible part of the two-dimensional Brillouin zone, we have used the special $\mathbf{k}$ point technique[50] (see Sec. III E).

III. RESULTS: ZENER CURRENT AND WANNIER-STARK RESONANCES IN INHOMOGENEOUS FIELDS

We consider a GaAs p-i-n junction with an intrinsic region of 20 nm and high n- and p-doping concentrations such that the Fermi level lies at the bottom of the conduction band on the n side and at the top of the valence band on the p side (with T=300 K, $n \simeq p \simeq 10^{19}$ cm^{-3}; see Fig. 2). For this situation, the built-in potential equals the energy gap. Hence, any externally applied reverse bias $[V_r = (U_R - U_L)/e]$ causes the conduction and valence bands to overlap which induces a tunneling current between the valence band in p-type region and the conduction band in the n-type region. We assume the electric field to be strictly parallel to the growth axis which we take to be the [001] direction. General field directions will be discussed in Sec. IV D.

In this paper, a tunneling coefficient or tunneling current from a given valence band on the p side into a particular conduction band at the n side always implies that these bands are in-channel states of the scattering states involved in the charge transport. Other bands might well be involved in the intermediate tunneling region but they are, strictly speaking, ill-defined due to the lack of translational invariance in the direction of the field.

The number of bands that contributes to the tunneling current depends on the applied bias. While the heavy-hole, light-hole, and first conduction band are always involved in the process, the split-off band only contributes if $eV_r > E_{so}$, where E_{so} is the split-off energy (= 0.3428 eV). In principle, electrons can tunnel into the second conduction band on the n side as soon as $eV_r > E(X_7^c) - E(\Gamma_6^c) = 0.92$ eV, but this indirect tun-

neling is very weak since the momentum $\Delta p = \hbar \Delta k$ provided by field-induced tunneling is of the order of the inverse width of the tunneling barrier, heF/E_{gap}. With fields of the order of 1 MV/cm, $\Delta k \approx 10^6$ cm^{-1} which is much smaller than the X-Γ separation in k space.

In Fig. 3 we show, as a function of the energy of an electron incident from the p region, the individual contributions to the transmission coefficient at $\mathbf{k}_{\|} = \mathbf{0}$ from each of the top valence band channels (heavy-hole, light-hole, split-off; denoted by v) into the first and second conduction band (denoted by c_1, c_2),

$$\sum_{i \in c_1, c_2} T_{(L, k_v^- \rightarrow R, k_i^+)}(\mathbf{k}_{\|} = \mathbf{0}, E).$$

Here, the total potential drop is $eV_D = eV_r + E_{\text{gap}} = 2.5$ eV corresponding to an applied bias of $V_r = 1.07$ V, and a field of $F = 1.25$ MV/cm. The zero of energy corresponds to the top of the valence band on the p side. The transmission coefficient is seen to be a fairly smooth function of energy except at the onset of the split-off band. In accord with WKB arguments for tunneling, the results show that the tunneling probability decreases exponentially with increasing electron mass. As a consequence, the Zener current that corresponds to this situation is dominated by the light-hole band, whereas the split-off band contributes only 10% to the total current.

In Fig. 4, we consider a different situation where the potential drop across the p-i-n structure is $V_D = 3.4$ V, corresponding to an applied reverse bias of $V_r = 1.95$ V. The figure depicts the transmission coefficient at $\mathbf{k}_{\|} = \mathbf{0}$, summed over all incoming valence band channels, for tunneling into the first or second conduction band. Initial electron band states that lie within 0.48 eV of the top of the valence band on the p side can tunnel into electron states of the second conduction band on the n side that lie above all states of the first conduction band. Indeed, the first conduction band width in the present tight-binding

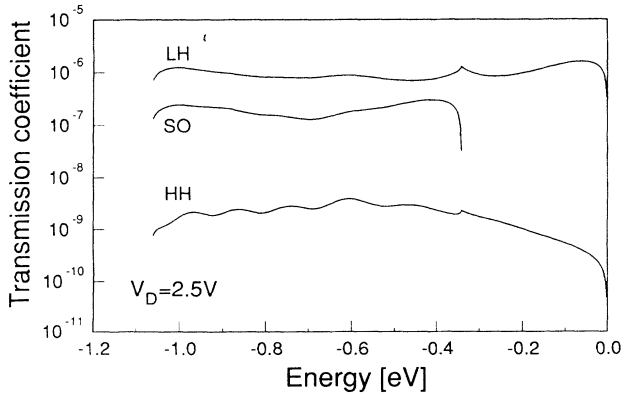

FIG. 3. Calculated transmission coefficients in a GaAs p-i-n structure with an intrinsic region of 20 nm. The abscissa shows the energy (in eV) of the incoming electron in the heavy (HH), light (LH) and split-off (SO) hole band, respectively. The final state lies in the conduction bands and $\mathbf{k}_{\|}$ is set to zero. V_D is the potential drop and the field is assumed constant in the intrinsic region and zero in the doped areas.

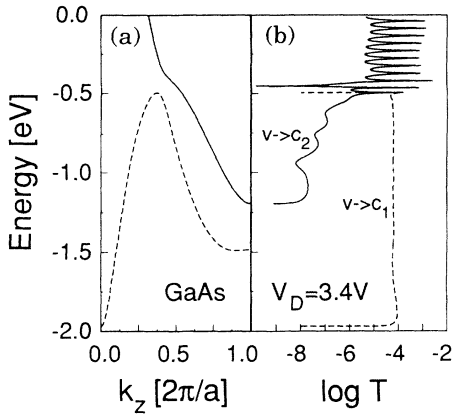

FIG. 4. (a) Energy band structure of first and second conduction bands along the [001] direction. (b) Calculated transmission coefficient for same p-i-n structure as in Fig. 3, summed over all in-channel states associated with hole bands and for $V_D = 3.4$ V. The out-channel states are associated with either the first (c_1) or second (c_2) conduction band. The logarithm is to base 10.

model is $\Delta_{c1} = 1.47$ eV and one has $eV_r - \Delta_{c1} = 0.48$ eV.[51]

Since a direct ($\Gamma \rightarrow \Gamma$) transition from the top of the valence band into the second conduction band requires an applied bias exceeding $E(\Gamma_7^c) - E(\Gamma_6^c) = 4.6$ eV, one may not expect significant contributions from tunneling into the second conduction band. In contrast, the results depicted in Fig. 4 show that the transmission coefficient is large and shows oscillations with a period very close to $eFa_{\perp} = eFa/2$ where $a_{\perp}$ is the lattice constant in the [001] direction. Electrons that have an initial energy further away from the valence band edge only tunnel into the first conduction band, with a smooth transmission rate and not displaying any oscillations.

In Fig. 5 we depict the current J and the conductance dJ/dV for the investigated diode as a function of the applied potential, calculated according to Eq. (12). For the $\mathbf{k}_{\|}$ integration, we divided the Brillouin zone into a spherical inner region with $|\mathbf{k}_{\|}| < 0.05\,(2\pi/a_{\|})$ and an outer region. For all relevant applied biases, only k states

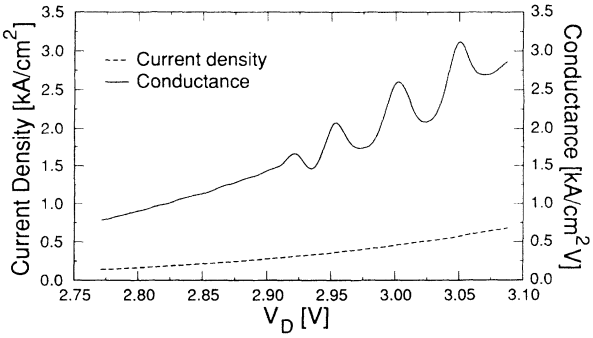

FIG. 5. Predicted current density and conductance for a 20 nm GaAs p-i-n diode as a function of the potential drop V_D in volts. The oscillations in the conductance reflect the presence of Wannier-Stark resonances.

in the inner region contribute to the current and tests have shown that between four and eight special **k** points in the irreducible part of the two-dimensional Brillouin zone give accurate results.

This Fig. 5 shows that, for biases larger than the threshold value $eV_D = \Delta_{c1} + E_{gap}$, the current shows oscillations that reflect the resonance peaks in the transmission coefficient, depicted in Fig. 4. As we will discuss in the subsequent sections, these oscillations reflect the Wannier-Stark resonances.

A. Interpretation: a simple one-band picture

In order to understand and interpret our results, we will proceed, in the first step, by considering a simple one-band tight-binding model that reflects some, but not all, of the essential qualitative properties of Wannier-Stark ladders.

We consider a finite open chain of N atoms described by the Hamiltonian

$$H = \sum_n \left[-t(c_n^\dagger c_{n+1} + c_n^\dagger c_{n-1}) + V_E(n) c_n^\dagger c_n\right], \quad (17)$$

where the hopping constant t gives a band width $\Delta = 4|t|$ and $c_n^\dagger$, c_n are the electron creation and annihilation operators, respectively. We label the atoms from 1 to N from left to right. For a concrete example, we choose $N = 50$. $V_E(n)$ is the externally applied potential and is taken to decrease linearly from its value zero for $n \leq 20$ to its minimum value $V_E(n) = -V_D$ for $n \geq 30$. V_D is the total potential drop across the chain. In terms of the electric field strength F and lattice constant a, we have $eV_D = 10eFa$ in our example. This defines three regions, in analogy to Fig. 2: there is a field-free "bulk-like" region L near the left end and a region R near the right end of the chain. The electric field is nonzero only in the middle region M. We note, however, that a finite chain does not allow for a finite steady-state current; however, here we are only interested in the electronic structure as a function of applied bias. Since $N \gg 1$, the energy spectrum differs only negligibly from a chain with periodic boundary conditions.

The energy spectrum of the Hamiltonian, Eq. (17), for different applied voltages is shown in Fig. 6, where we depict the energy of all eigenstates as a function of the level number. Level number 1, for example, corresponds to the highest energy in the L region. The hopping term has been set to $t = -1$. For zero applied bias, [Fig. 6(a)], the band structure exhibits the well-known cosine function and all wave functions are spread out over the whole chain.

Already a small applied potential totally alters the character of the eigenstates: (i) the energetically lowest lying states ($-\Delta/2 \geq E \geq -\Delta/2 - eV_D$) form extended band states in region R, but decay exponentially into region M; (ii) the highest lying states ($\Delta/2 \geq E \geq \Delta/2 - eV_D$) are extended "bulk-like" states in region L and decay exponentially into the right region M; (iii) the states in the central energy range ($\Delta/2 - eV_D \geq E \geq -\Delta/2$) extend into all three regions and stay delocalized.

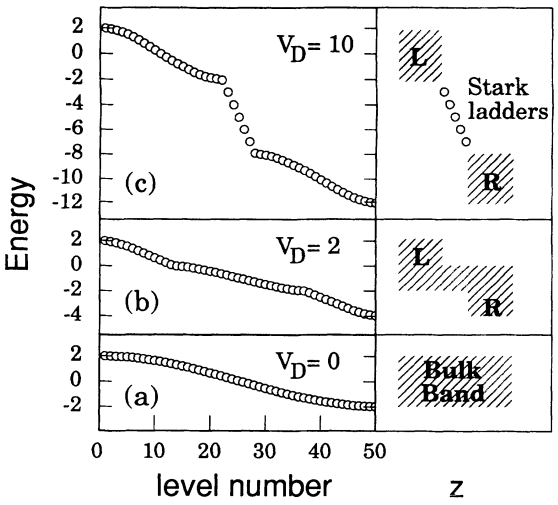

FIG. 6. *Left panel:* Calculated energy levels, in units of t, of a one-band tight-binding Hamiltonian as a function of the energy level number and for several potential drops. There are 50 lattice sites and the field is constant and nonzero only between the 20th and 30th lattice sites. *Right panel:* Schematic local energy band picture corresponding to the potential drop in the left panel. When V_D exceeds the band width, localized Wannier-Stark states form.

The electric field can be thought of as producing a position dependent band structure $E(x)$ that has the same width Δ at each position $x = na$ but a band center energy that is lowered by the potential drop eFa on neighboring sites [see right side of Fig. 6(b)]. The point is that only states of the same energy can couple with one another. Since only the states in the middle energy range overlap with all band states $E(x)$, these states are delocalized over the whole chain.

Once the applied potential eV_D exceeds the band width Δ, the eigenstates of H in the field regime M become localized, as shown in Fig. 6(c). In this case, the field breaks the bonds.[52] In Fig. 7 we show the site occupancies for the 5th, the 25th, and the 45th levels of the chain,

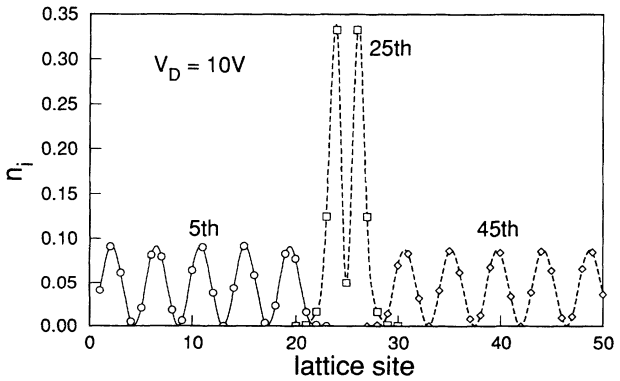

FIG. 7. Site occupancies of the 5th, 25th, and 45th eigenstates of the one-band model. The field corresponds to the situation in Fig. 6(c). The 25th state is a Wannier-Stark state, whereas the 5th and the 45th are semibulk states.

respectively, corresponding to the situation in Fig. 6(c). They have been interconnected only to guide the eye and clearly show the localization in the central region. These localized states are the one-band WS ladder states. In the present one-band model, the maximum number of localized WS states obviously equals the number of atoms in field region M. The energy separation ΔE between these WS states approaches eFa exponentially as a function of the potential drop.

B. Full band calculation of nonpropagating states

In this section we return to the full band multichannel scattering theoretic analysis of the GaAs p-i-n diode in order to interpret the origin of the resonances in the current in Fig. 5. As explained in Sec. II E, a bound state in the transfer matrix formalism is characterized by the condition that $|\det(\mathbf{P}^{-+}(\mathbf{k}_{\|}, E))| = 0$. Resonances or quasilocalized states that interact with energetically degenerate extended states can be identified from minima of $|\det(\mathbf{P}^{-+})|$. Figure 8 shows $|\det(\mathbf{P}^{-+}(\mathbf{0}, E))|$ as a function of the energy for various applied voltages for a p-i-n junction with an i zone of 5.4 nm. The band edges of the top valence band, first and second conduction band, tilted according to the applied field, are schematically shown in Fig. 9. Energy zero is at the top of the valence band in the left (p doped) region L. First, we consider $V_D = 1$ V [see Fig. 9(a)]. For this voltage, the determinant is a fairly smooth function of the energy. No localized states are present. The onset of each band edge induces some structure in $|\det(\mathbf{P}^{-+})|$ due to an increase in the density of states.

Next we consider a voltage drop of $V_D = 2.5$ V [Fig. 9 (b)]. Figure 8 shows that the $|\det(\mathbf{P}^{-+})|$ has pronounced periodic minima for energies $E_{\text{gap}} > E > E_{\text{gap}} - (eV_D - \Delta_{c1}) = 0.4$ eV, where Δ_{c1} is the width of the first conduction band. In this energy range, there are electronic states associated with the first conduction band in the central region M that do not overlap energetically with any of the semibulk states of the first conduction band in the L and R region, as can be deduced from Fig. 9(b). This allows the formation of localized WS states which are superpositions of all Bloch states of the first conduction band. In contrast to the one-band picture of the last section, however, these WS states do not form strictly localized (bound) states, since they are in resonance with the extended semi-Bloch states of the second conduction band of the right region R. The fact that the WS states overlap with some semibulk states associated with other bands explains why the determinant $|\det(\mathbf{P}^{-+})|$ merely has minima, rather than zeros.

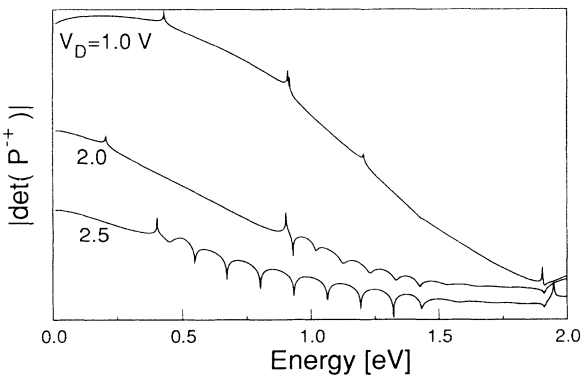

FIG. 8. Calculated determinant of the transfer matrix element P^{-+} as a function of energy for a GaAs p-i-n structure with an intrinsic zone of 5.4 nm width and for $\mathbf{k}_{\|} = \mathbf{0}$. The equally spaced minima in the determinant reflect the presence of WS resonances associated with the first conduction band and appear for $V_D > \Delta_{c1}$.

For energies outside the energy range $0.4 < E < 1.43$ eV, for $V_D = 2.5$ V, the electronic states of the first conduction band in the M region overlap with band states of the same band in the asymptotic semibulk L or R regions. This prevents the formation of localized WS states and gives a smooth energy dependence of the determinant, as well as the transmission coefficients (see Fig. 3).

For voltage drops that are smaller than the band width of the first conduction band, $eV_D < \Delta_{c1}$, all band states of the first conduction band in the M region overlap with extended (first conduction band) states in one of the contact regions. Consequently, no WS states form, as can be seen for $V_D = 1$ V in Figs. 8 and 9.

The energy separation between WS states is approximately equidistant and equal to $eFa_{\perp}$. In contrast to uniform field models, we find some deviations due to the finite spatial extent of the electric field and due to the multiband character of the scattering states. For long intrinsic regions and large potential drops, however, the energy separation tends towards the asymptotic value $eFa_{\perp}$.

C. Quantitative criteria for Wannier-Stark resonances

We can now condense the results of the present calculations in the following conditions for the appearance of signatures of WS resonances in the electric current through semiconductors.

There are two conditions that must be met in order to obtain oscillations in the interband tunneling current as a function of the applied voltage that are caused by the formation of WS resonances.

(1) An energy band can support Wannier-Stark ladder resonances only if the total potential drop eV_D across the semiconductor exceeds the total zero-field band width Δ of that band in field direction.

(2) Oscillatory I-V characteristics due to interband tunneling is obtained only if at least three different electronic energy bands participate in the tunneling process: there is one band through which the electron enters the field region (in-channel or "emitter" band), there is another band into which the electron tunnels and leaves the device (out-channel or "collector" band), and there must be a third band that produces the Wannier-Stark resonances, that resonantly enhances the tunneling process from the in-channel to the out-channel band.

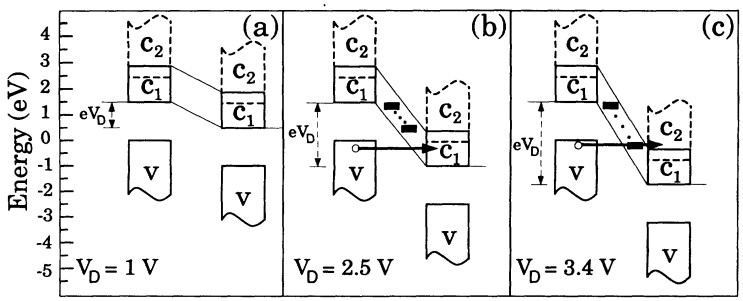

FIG. 9. Schematic band picture of a GaAs p-i-n diode, illustrating the origin of Wannier-Stark resonances in the Zener tunneling current. (a) No WS resonances form when the potential drop is smaller than the first conduction band width Δ_{c1}. In addition, there is no Zener tunneling in this case since $V_D < E_{\rm gap}$. (b) When V_D exceeds the first conduction band width, one obtains WS resonances of finite width that are associated with the first conduction band (thick bars). The WS resonances do not overlap in energy with the extended semibulk states associated with the first conduction band in the right region and, therefore, cannot contribute to the (elastic) Zener tunneling current. (c) For $V_D = 3.4$ V ($eV_D > E_{\rm gap} + \Delta_{c1}$), WS states resonantly enhance the tunneling current from the valence band to the second conduction band and produce oscillations in the current as a function of V_D.

If the first condition is not satisfied, the states in this band are propagating, delocalized states that extend into the contact regions. As a consequence, no WS ladder resonances form. Whenever $eV_D > \Delta$, on the other hand, there is a barrier provided either by an energy gap or small interband matrix elements, Eq. (3), that prevents the delocalization of the WS resonances.

In fact, the first condition resembles the semiclassical picture of Bloch oscillations. If we interpret the tunneling states in the field region in terms of tilted Bloch states (which is rigorously[52,13] justifiable), the first condition guarantees that the electron tunnels through *all* zero-field Bloch states at a given energy [see Fig. 9(b)].

The second criterion is nothing but a condition for resonant tunneling. It implies that the in-channel states, the localized WS resonances, and the out-channel states must be energetically aligned. The first condition is met for the first conduction band of GaAs for the applied voltages shown in Fig. 9(b) and (c). However, the second condition is only fulfilled in Fig. 9(c) where the electron tunnels from the valence band into the second conduction band and the first conduction band provides localized WS resonances. These resonances also form for the situation in Fig. 9(b), but there is no energy conserving tunneling process that connects the asymptotic scattering states with the WS resonances.

In optical experiments, the first condition suffices to observe WS resonances. In a transport experiment, however, the second condition must also be fulfilled.

These results lead us to the conclusion that the oscillations in the tunneling current that have been observed experimentally for very low applied bias in InSb p-n structures several years ago cannot be due to WS resonances.[16] The same conclusion has been reached before by Argyres.[26]

These conditions lead to a new classification of interband tunneling processes: There are two regimes: (i) the *Zener regime* where no WS resonances appear in the current and (ii) the *Stark regime* where the above conditions (1) and (2) are satisfied and the I-V characteristics contain oscillatory contributions (Fig. 5).

D. Wannier-Stark ladder assisted indirect tunneling

In Fig. 4, we have shown that WS resonances originating from the first conduction band resonantly enhance the interband tunneling from the top valence band states into the lowest band states of the *second* conduction band of GaAs [cf. Figs. 9 (c)]. Since the latter band states lie in the middle of the Brillouin zone, the momentum of the incoming and outgoing scattering states is very different. This raises the question which mechanism provides this momentum transfer since the calculation incorporates neither phonons nor impurities.

The Zener current between states of different momentum is indeed negligible as long as no WS resonances form. This can be seen clearly from the transmission coefficient $T_{v\to c2}$ for energies smaller than -0.48 eV in Fig. 4. Efficient interband tunneling only occurs for energies between $-0.48 < E < 0$ eV, i.e., in the WS regime.

This finding can be understood in terms of "WS ladder assisted tunneling." A WS resonance ν is a linear combination of all zero-field Bloch states $|\mathbf{k}_{||}, k_z\rangle$ with fixed $\mathbf{k}_{||}$ associated with an energy band and is spatially localized. Indeed, within the one-band and homogeneous-field approximation, one has $|\langle \mathbf{k}_{||}, k_z|\nu, \mathbf{k}_{||}\rangle|^2 = |\mathbf{G}|^{-1}$. Here, $|\mathbf{G}|$ is the shortest reciprocal lattice vector in the direction of the field.[53] This localization provides the momentum for indirect tunneling, analogously to impurity-assisted carrier recombination.

E. Zener tunneling rate: theory and experiment

In this section we present numerical results for the Zener current in the low bias Zener regime. In Fig. 10

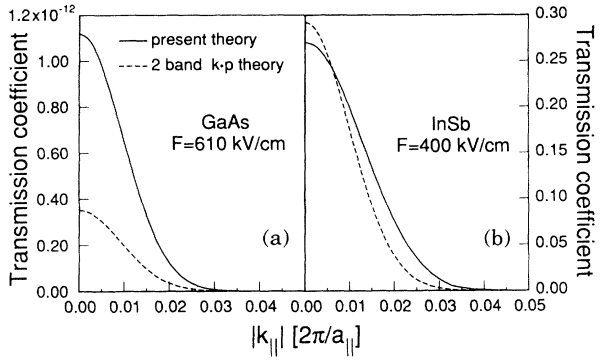

FIG. 10. Calculated energy-averaged Zener tunneling coefficient for (a) a GaAs and (b) an InSb p-i-n diode (20 nm i zone) as a function of $|\mathbf{k}_{\|}|$. The electric fields F are indicated in the figure. The present full-band multichannel results are compared to the widely used two-band $\mathbf{k}\cdot\mathbf{p}$ model of Kane (Ref. 24). The high value of the transmission coefficient in InSb originates in the small band gap.

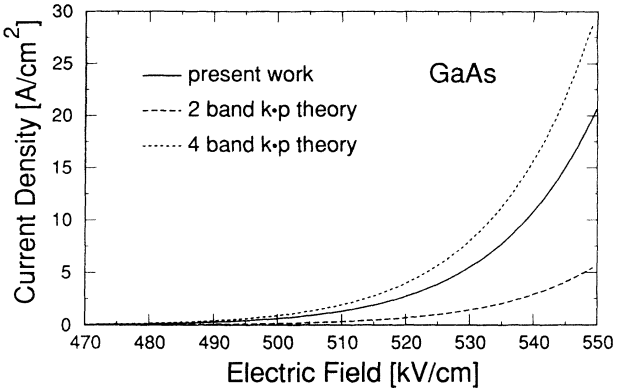

FIG. 12. Comparison between the present calculation of the Zener tunneling current and the analytical two-band and four-band $\mathbf{k}\cdot\mathbf{p}$ models of Refs. 24 and 57, respectively.

we plot the total tunneling transmission coefficient T in GaAs and InSb as a function of $\mathbf{k}_{\|}^2$. Since the energy dependence of T is weak (see Fig. 3), we have taken an average over energy,

$$\frac{1}{eV_r}\int_0^{eV_r} dE \sum_{j\in v}\sum_{i\in c_1,c_2} T_{(L,k_j^-)\rightarrow(R,k_i^+)}(\mathbf{k}_{\|}=0,E).$$

Even a small increase in $\mathbf{k}_{\|}$ leads to an exponential decrease in the tunneling probability. This decrease originates in two effects, namely an increase in the fundamental energy gap and an increase of the effective mass due to nonparabolicity effects.

In Fig. 11, we compare the predicted Zener current of the present model with experimental results[54] for a GaAs p-i-n structure with $n = 10^{19}$ cm^{-3}, $p = 2\times10^{19}$ cm^{-3}, and an intrinsic region of 18 nm. Excellent agreement is found in the voltage regime below the avalanche threshold.

In Fig. 12 we show the predicted Zener current [Eq. (12)] in a GaAs p-i-n diode, with a doping concentration of $n = p = 10^{18}$ cm^{-3} and a 40 nm intrinsic zone. Also, we compare the present results in Figs. 10 and 12 with the analytical model of Kane that is based on expression Eq. (4). Kane's results for GaAs are significantly smaller than the present ones and also underestimate the experimental data.[55,56] Nevertheless, it is interesting to note that the full-band results for the Zener current can be reasonably well reproduced by a WKB-type analytical expression of the form of Eq. (4), provided the effective mass is replaced by a more accurate four-band $\mathbf{k}\cdot\mathbf{p}$ result,[57]

$$m^* = \frac{\hbar^2}{2}\frac{\frac{1}{2}+\frac{E_{so}}{E_g}}{(\frac{1}{2}+\frac{2}{3}\frac{E_{so}}{E_g})(b-c)+a(\frac{1}{2}+\frac{E_{so}}{E_g})}, \tag{18}$$

where

$$a = \frac{\hbar^2}{4}\left(m_c^{-1}+m_{hh}^{-1}\right) - \frac{3\hbar^2}{8E_{so}}\left(m_{lh}^{-1}+m_{hh}^{-1}-2m_{so}^{-1}\right) \times\left(E_g+\frac{2E_{so}}{3}\right),$$

$$b = \frac{3\hbar^2(E_g+E_{so})}{4E_{so}}\left(m_{lh}^{-1}+m_{hh}^{-1}-2m_{so}^{-1}\right),$$

$$c = \frac{3\hbar^2}{8E_{so}}\left[E_g(m_{lh}^{-1}-m_{hh}^{-1}) - 2(E_g+E_{so}) \times(m_{so}^{-1}-m_{hh}^{-1})\right].$$

Here, m_c denotes the first conduction band mass and m_{hh}, m_{lh}, m_{so} are the heavy-hole, light-hole, split-off masses, respectively. All these masses are taken from the experimental data at the Γ point. For GaAs, one gets $m^* = 0.0615$.

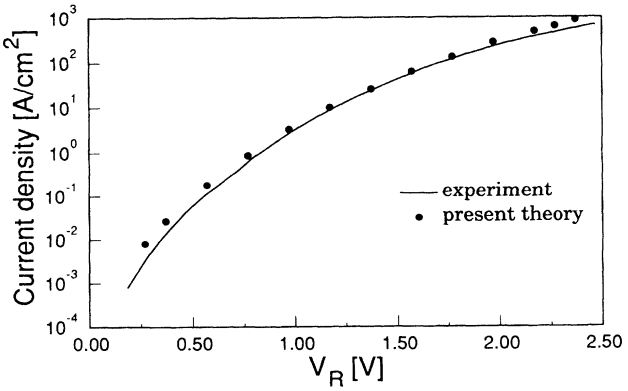

FIG. 11. Comparison between the experimental and calculated tunneling current density as a function of the reverse bias for a GaAs p-i-n structure with an 18nm i zone, and doping concentration of n=10^{19} cm^{-3} and p=2×10^{19} cm^{-3}.

IV. CAN WANNIER-STARK LADDERS BE OBSERVED IN BULK TRANSPORT?

An interesting prediction that is emerging from the results of the previous sections is the feasibility of detecting

WS resonances in bulk transport experiments, in contrast to what has been widely believed. Historically, the search for these resonances in bulk material was bound to be unsuccessful since the stringent sample requirements can only be satisfied by very specific molecular-beam-epitaxially grown structures. The present calculations predict the following prerequisites for observing oscillations in the electric current due to WS states.

First, the n- and p-doping concentration should be sufficiently high so that the potential drop occurs predominantly in the intrinsic zone. In GaAs, this implies $n,p > 10^{18}$ cm^{-3} at liquid nitrogen temperatures. Second, the potential drop must exceed the band gap plus the width of the first conduction band. This condition requires $V_D > 3.4$ V for fields along the [001] direction, or $V_D > 2.5$ V along the [111] direction. In GaAs, the maximum fields that can be reached experimentally lie between 1 and 2 MV/cm. In fact, p-i-n diodes have recently been fabricated[56,54] with a length of the i zone $w_i = 18$ nm that show a breakdown voltage of 4 V, corresponding to a maximum field of $F_{\max} = 1.91$ MV/cm. Consequently, the width of the i zone must satisfy the condition $w_i > V_D/F_{\max} \approx 20$ nm. Third, the width w_i should simultaneously be as short as possible to give a measurable tunneling current and a large separation energy eFa between WS levels. Within the analytical two-band $\mathbf{k}\cdot\mathbf{p}$ model discussed in Secs. I and III E, the current density scales exponentially with w_i and is approximately given by

$$J = \frac{e^3 V_D^2}{18\pi w_i \hbar^2}\sqrt{\frac{m^*}{2E_g}}\exp\left\{-\frac{\pi w_i\sqrt{m^* E_g^3}}{2\hbar e V_D}\right\}.$$

For $V_D = 3$ V and a 20-nm intrinsic zone, this gives $J = 1$ A cm^{-2}.

The crucial point is that these conditions can be met before avalanche breakdown due to impact ionization occurs. Clearly, there are additional factors that contribute to a broadening of WS resonances such as electronic band mixing effects, interface roughness and phonon scattering, or the misalignment of the electric field relative to a crystal axis. We are going to critically examine these effects in this section. It turns out that the exponential dependence of the tunneling current on any energy barrier height and width is a very favorable effect that stabilizes the formation of sharp WS resonances.

A. Electronic effects

As shown in Sec. II D, the Zener tunneling current contains an integral over $\mathbf{k}_\parallel$. The positions of the WS resonances shift rigidly in energy with $\mathbf{k}_\parallel$ by some offset that is approximately given by $\langle\varepsilon_{\mathbf{k}}\rangle$ in Eq. (1). This offset is a function of $\mathbf{k}_\parallel$. If all $\mathbf{k}_\parallel$ contribute to the current with equal weight, the WS states would overlap each other and could not be observed. Actually, however, the WS states that contribute to the resonant interband tunneling current are dominantly states with $\mathbf{k}_\parallel \approx 0$. This can be seen from Fig. 13, where we show the total transmission

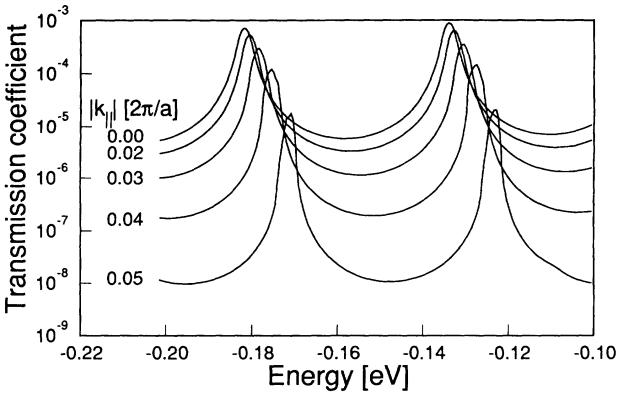

FIG. 13. Dependence of the interband Zener tunneling coefficient on the electron wave vector $\mathbf{k}_\parallel$, plotted as a function of initial electron energy. The structure and the bias condition is the same as in Fig. 4. The transmission maxima correspond to WS resonances and exponentially decrease with increasing $\mathbf{k}_\parallel$, i.e., away from the band edges.

coefficient $T_{(L,v\to R,c)}(\mathbf{k}_\parallel, E)$, summed over all incoming valence band and outgoing conduction band states, as a function of energy for different $\mathbf{k}_\parallel$. The doping and applied bias in this figure is the same as in Fig. 4. As we have already pointed out, the increasing gap causes the tunneling probability to decrease very strongly with $\mathbf{k}_\parallel$. Consequently, the WS resonances can still be clearly resolved.

B. Phonons and interface roughness

WS resonances can only be observed if their width Γ is smaller than their energy separation. The dominant broadening of Wannier-Stark resonances can be expected to originate in phonon scattering, assuming sufficiently pure and homogeneous samples. The WS level broadening due to optical and acoustic phonon scattering has been estimated to be of the order of 5 meV in standard bulk semiconductors at low temperature and strong electric fields.[58] This value is well below the energy separation of up to 50 meV between WS resonances for intrinsic zone widths less than 20 nm such as depicted in Fig. 5. It also corresponds to a scattering time of the order of 100 fs that is typical for GaAs. Alternatively, for a crude estimate, one may think of a phonon to modulate the nearest-neighbor distance by an amount $\delta a \ll a$ giving a width of the WS ladders of the order of $eF\delta a \ll eFa$.

Phonons open additional channels for tunneling processes since in- and out-channel states can have energies that differ by integer multiples of the phonon energies. These processes will show up as additional resonances in the current, in addition to the ones we have analyzed in the previous sections. Indeed, phonon-assisted tunneling was studied in Refs. 53, 24, and 59–61. These calculations revealed, however, that the phonon-assisted tunneling probability is at least three orders of magnitude smaller than the direct electronic tunneling process

so that they are not likely to blur the elastic WS resonances.

Finally, interface roughness or inhomogeneous lateral doping profiles yield a local shift of the threshold voltage beyond which WS resonances form and, more importantly, influence the position of WS resonances in the energy spectrum as a function of position. This has a similar effect as the superposition of different $\mathbf{k}_{\|}$ states which was discussed above. The measured current is an average over the cross section of the *n-i-p* structure. The current maxima will be produced by the WS states in the region(s) of maximum electric field. Again, the exponential dependence of the tunneling current on the field or, equivalently, the tunneling distance will tend to suppress any signals other than those from the region of maximum electric field. However, if lateral field inhomogeneities become large the peak-current contributions from lower-field regions may fall into the valley regions of the current contribution from the maximum-field region. Moreover, the maximum-field region may be small compared to the total cross section of the diode. This indicates that high lateral-field uniformity in the maximum-field region is highly desirable.

It should be noted that these considerations are analogous to those for resonant-tunneling (RT) structures, where subsidiary minima due to LO phonon emission have been found to be rather weak.[62] We are not aware of any quantitative study of the effect of interface roughness or layer-width fluctuations based on a three-dimensional model for RT structures. A qualitative discussion of layer-width fluctuations based on a one-dimensional model for the RT system can be found in Ref. 63. Due to the low carrier densities in the high-field region of the *n-i-p* diode, the Coulomb interaction, however, can be expected to be of a lesser importance than for tunneling processes in conventional semiconductor heterostructures.

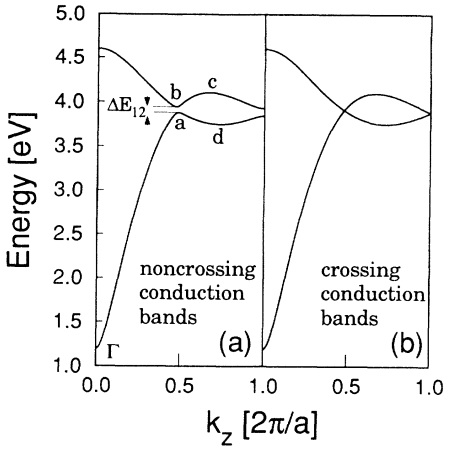

FIG. 14. Topology of overlapping conduction bands in the [001] direction. The left panel shows a noncrossing band situation that is typical for ZnS-type semiconductors (T_d^2 group). In the right panel, the two conduction bands do not interact and cross each other, such as in a diamond structure (O_h^7 group).

C. Interband coupling

As explained earlier, an energy band can support WS ladder resonances only if $eV_D > \Delta$ where Δ is the zero-field band width. Since all conduction bands overlap and many bands cross each other in a three-dimensional semiconductor, there has been a controversy about whether WS ladder resonances form at all in a realistic many-band situation of a semiconductor. In particular, it has been argued that strong interband coupling suppresses the formation of WS resonances in the tunneling current.[29]

In order to investigate the effect of band crossing, we have performed a model study based on a sp^3s^* tight-binding approach. Starting from the electronic structure of Ge, a typical nonpolar semiconductor, we systematically changed the anion-*s* and cation-*s* on-site orbital energies to open a gap along the [001] direction between the two lowest conduction bands, as shown in Fig. 14(a) and 14(b).

We consider a *p-i-n* structure with an *i* zone of 56 nm (F = 0.8 MV/cm) and a potential drop of V_D = 4.4 V. This structure supports WS states associated with the lowest conduction band. The transmission coefficient for three different values of the energy separation ΔE_{12} between the first and second conduction band (Fig. 14) is shown in Fig. 15. It depicts the total transmission coefficient as a function of the outgoing electron energy.

For ΔE_{12} = 48 meV, the tunneling current from the valence band to the second conduction band shows WS resonances that originate from the first conduction band, in analogy to the results of Sec. III. The transmission coefficient is zero in the energy regime corresponding to the gap between first and second conduction band, marked by the points *a* and *b* in Fig. 14.

For smaller energy separation $\Delta E_{12} \to 0$, the WS resonances tend to disappear, since an electron can tunnel

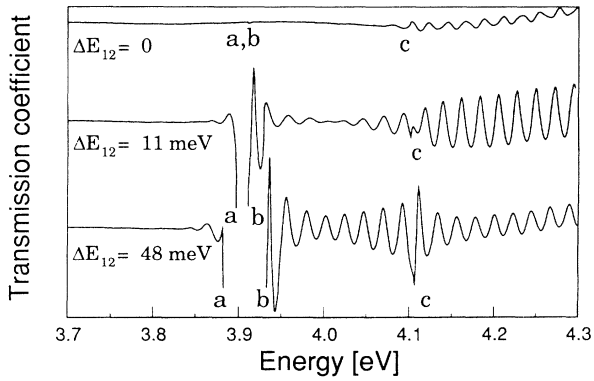

FIG. 15. Transmission coefficient for tunneling from the valence bands into the conduction bands shown in Fig. 14, plotted as a function of the outgoing conduction band electron energy, for $\mathbf{k}_{\|} = 0$. The letters a, b, c refer to the energy band positions specified in Fig. 14. The figure illustrates the suppression of the WS resonances with diminishing conduction band splitting ΔE_{12}.

directly from the first into the second conduction band [i.e., from a to b in Fig. 14(a)]. Effectively, both conduction bands start to form one single band. Only for final electron energies exceeding the maximum of the first conduction band [c in Fig. 14(a)], WS resonances appear irrespective of the value of ΔE_{12}.

One can also explain this behavior in the semiclassical Bloch oscillation picture. The electron cycles through all k values of a given band, which is the first conduction band in this case. For small ΔE_{12}, however, the electron can tunnel into a higher band before it reaches the boundary of the Brillouin zone and this destroys the WS oscillations.

Thus, the crucial point is that the formation of WS resonances in the tunneling current is not sensitive to the topological definition of an energy band. Furthermore, interband tunneling does not smear out the WS resonances of an energy band that is separated from neighboring bands by ΔE of the order of 10 meV for each value of k_z across the Brillouin zone. This holds for fields up to ~ 1 MV/cm.

D. Wannier-Stark ladders in misaligned fields

For a one-band model and the uniform field approximation, the energy separation between WS ladders is $eF\,2\pi/|G|$, where $|G|$ is the shortest reciprocal lattice vector in field direction. This result seems to imply a dramatic instability of WS ladders: an infinitesimal tilt of the electric field with respect to a crystal axis causes the lattice constant in the field direction to become nearly infinite and consequently to the loss of WS ladder states.

This sudden disappearance of WS levels is an artifact of the uniform field approximation as has been realized by many authors.[7,15] It has been pointed out, for example, that one can define physical observables, such as an averaged density of states, that are smooth functions of the direction of the field.[15] Some experiments,[17] however, have been incorrectly based on a literal interpretation of the uniform field result.

For a discussion of misalignment effects, it is mandatory to take into account the finite potential drop across any real semiconductor with contacts. In order to understand the predominant effects of field misalignment on the crystalline eigenstates, it is clarifying to study a finite two-dimensional electron system in terms of a one-band tight-binding model. Consider the Hamiltonian

$$H = \sum_{i,j} V_{i,j} a^{\dagger}_{i,j} a_{i,j} - t\, a^{\dagger}_{i,j}(a_{i+1,j} + a_{i-1,j} + a_{i,j+1} + a_{i,j-1}). \quad (19)$$

where $a^{\dagger}_{ij}$ (a_{ij}) denotes the electron creation (annihilation) operator on site ij, t is the hopping matrix element and $V_{i,j}$ is the electric potential. The potential is given by

$$V_{i,j} = eF_x x_i + eF_y y_j,$$

where x_i ($i = 1, N_x$) and y_j ($j = 1, N_y$) are the lattice vectors in the x and y directions, respectively, and we assume x to be the principal direction of the electric field, $F_x \gg F_y$.

We use a two-dimensional lattice cluster consisting of $N_x = 60$ and $N_y = 20$ sites which is simply truncated at its boundaries (equivalent to infinite walls), and a constant electric field F such that $eF_x a/t = 11$, where a is the lattice constant. The smallest tilt of the electric field that points towards a lattice point in this lattice is obviously $\theta_{\min} = F_y/F_x = 1/60$.

The electric field F_x is large enough to support localized WS ladder states in the x direction since the potential drop $eF_x N_x a$ is much bigger than the band width $4t$. In fact, the localization length of the WS states is of the order of one lattice constant. In Fig. 16 we plot the eigenvalues of the Hamiltonian Eq. (19) for different misalignments, as measured by the ratio of (F_y/F_x). Since we have chosen $eF_x a$ to be larger than the zero-field band dispersion in Fig. 16, the WS level states can be clearly identified. The eigenstates of the system are localized WS states in the x direction but completely delocalized Bloch-like states in the y direction as long as $eF_y N_y a \ll 4t$. As a consequence, a small misalignment of the field with $F_y \ll F_x$ has little effect on the character of the states along the x direction.

The crucial point we would like to stress is that the WS level spacing does not change abruptly to reflect a new periodicity whenever F_y/F_x points to another lattice vector. Indeed, the spectra shown in Fig. 16 do not change significantly when $F_y/F_x = \theta_{\min}$, in contrast to the prediction of the uniform field approximation. Only when F_y becomes large enough to support WS ladders by itself, the spectrum changes qualitatively. This clearly shows that WS states are stable with respect to small-field misalignments in any real material with a finite potential drop.

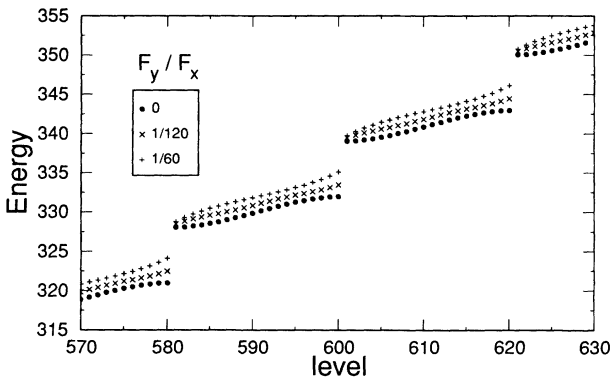

FIG. 16. Energies of a two-dimensional one-band tight-binding Hamiltonian in a constant electric field **F** with components F_x and F_y, in units of t. The figure shows a representative part of the spectrum. The lattice consists of 60 and 20 sites in the x and y directions, respectively. The WS levels do not change qualitatively with the direction of the electric field, even when **F** points to the lattice vector $F_y/F_x = 1/60$, provided the potential drop in the y direction is smaller than the band width.

V. CONCLUSIONS

We have first developed and adapted a general approach for the computation of the steady-state current response of general mesoscopic electronic device structures within elastic scattering theory. In particular, we have provided a general proof of orthogonality of scattering states for standard mesoscopic device structures. This proof holds both for a large class of potentials which assume a constant value or display a periodic behavior in the asymptotic regions. Completeness of scattering and bound states and unitarity of the S matrix follow from standard concepts of time-dependent scattering theory. We have shown that scattering theory, in conjunction with linear response, yields a conductance which is proportional to the transmission coefficient T of the system, rather than $T/(1-T)$. Furthermore, the range of validity of linear response for finite applied bias and proper construction of reservoirs have been addressed. Finally, this approach was applied to a three-dimensional model for the Zener diode.

Second, we have provided a conceptual framework and quantitative criteria for the occurrence of Wannier-Stark resonances in the interband tunneling current in semiconductors. We have focused on bulk semiconductors, even though the conceptual framework developed in this paper applies equally to superlattices.

We predict that WS resonances can be observed in realistic bulk p-i-n diodes since neither impact ionization, line width broadening, interband coupling, nor field misalignment is likely to smear out the resonances at low temperatures.

WS resonances associated with an electronic band only form when the potential drop across the device exceeds the band width. In contrast to the situation in optical experiments, we find that this condition does not suffice to obtain WS related oscillations in the dc tunneling current as a function of the applied voltage. In order to have WS ladder states resonantly enhance the interband tunneling current, the electric field must be strong enough to align a WS ladder state associated with a particular band with *two other bands*, one associated with the semi-infinite n-doped region, the other with the semi-infinite p-doped region.

We have shown that there are two regimes for the tunneling current in a p-i-n structure: a low-field or Zener regime where the conductance is a smooth function of the applied voltage V_r and a high-field or Stark regime where the conductance shows equally spaced oscillations due to WS resonances. The presence of these two regimes allows an unambiguous experimental identification of this effect.

ACKNOWLEDGMENTS

This work has been supported by the Deutsche Forschungsgemeinschaft (SFB 348), by Siemens Corporation, and the U.S. Army Research Office (W.P.). We gratefully acknowledge helpful and clarifying discussions with Drs. J. A. Majewski, G. Döhler, C. Hamaguchi, P. Lugli, and J. Schulman. W.P. also wishes to acknowledge hospitality received at the Walter Schottky Institute, TU-München, and the University of Graz, Austria.

APPENDIX A: THE DENSITY OPERATOR

Construction of the steady-state density operator is the key issue in deriving an expression for the steady-state current response of an electronic system. Here we use an adiabatic switching method which is closely related to the construction of stationary scattering states.[39,64] Starting from thermal equilibrium of the system in the distant past $t_o \ll 0$ and adiabatically "feeding" in the applied bias U one obtains, at $t=0$, a steady-state solution

$$\rho(0) = \lim_{\eta\to 0_+} \rho(0)^{(\eta)} = \lim_{\eta\to 0_+} \eta \int_{-\infty}^{0} dt e^{\eta t} \exp\{itH/\hbar\}\rho_o \exp\{-itH/\hbar\}, \tag{A1}$$

to a von Neumann equation for the system, where $H = H_o + U$ denotes the steady-state Hamilton operator and ρ_o is given in (6).

$\rho(0)$ may be found formally by solving a von Neumann equation into which a small (non-Hermitian) source term was added to account for dissipative action of a bath. Validity of the latter requires small deviation of $\rho(t)$ from ρ_o. Integration by parts shows that this procedure corresponds to a specific prescription of how to perform the limit $t_o \to -\infty$ in (A1).[39] Technically this construction is equivalent to a construction of scattering states due to Gell-Mann and Goldberger.[65,39,66]

Inserting the resolution of the identity expressed via the eigenkets of H into (A1) gives

$$\rho(0) = \int \sum_{N,N',E_N=E_{N'}} |N\rangle F_{N,N'} \langle N'|, \tag{A2}$$

with matrix elements

$$F_{N,N'} = \langle N|\rho_o|N'\rangle = \int \sum_{\nu} f_\nu \langle N|\nu\rangle\langle\nu|N'\rangle.$$

Here, $|N\rangle$ and $|\nu\rangle$ are a short-hand notation for the eigenstates of H and H_o, respectively. Calculation of the steady-state density operator thus requires knowledge of ρ_o and the overlap between eigenstates of H_o and H. It is apparent from (A2) that there must be a perturbative connection between the basis states of H_o and H for this construction to be successful. This is in analogy to the Gell-Mann-Low theorem which provides an alternative means to construct the density operator.[67] For a detailed discussion of this procedure we refer to the literature.[39,65]

APPENDIX B: LINEAR RESPONSE

Here we give a simple derivation of the steady-state density operator within linear-response theory (Kubo for-

malism) which allows a discussion of its regime of validity. Applied to the current response of the system, it leads to a Landauer-type, or rather, $\sigma \propto T$ conductance. Furthermore, it will be seen that following standard scattering theory avoids any confusion regarding the order in which limits have to be taken.[36] Here, it is, of course, assumed that H and H_o are related perturbatively to one another.

Within linear response regarding the applied potential $U = H - H_o$, above expression for $\rho(0)$, (A1) may be simplified

$$\begin{aligned}\rho(0) &= \lim_{\eta\to 0_+}\eta\int\sum_\nu f_\nu\int_{-\infty}^0 dt' e^{\eta t'}\mathcal{U}_w^\nu(0,t')|\nu\rangle\langle\nu|\mathcal{U}_w^\nu(0,t')^{-1}\\ &= \lim_{\eta\to 0_+}\eta\int\sum_\nu f_\nu\int_{-\infty}^0 dt' e^{\eta t'}\left(1+\frac{i}{\hbar}\int_0^{t'}dt'' U_w^\nu(t'')\right)|\nu\rangle\langle\nu|\left(1-\frac{i}{\hbar}\int_0^{t'}dt'' U_w^\nu(t'')\right)+O(U^2)\\ &= \int\sum_\nu f_\nu \lim_{\eta\to 0_+}\eta\int_{-\infty}^0 dt\, e^{\eta t}\mathcal{U}_w^\nu(0,t)|\nu\rangle\langle\nu|\lim_{\eta'\to 0_+}\eta'\int_{-\infty}^0 dt' e^{\eta' t'}\mathcal{U}_w^\nu(0,t')^{-1}+O(U^2)\\ &= \int\sum_\nu f_\nu|\nu^+\rangle\langle\nu^+|+O(U^2),\end{aligned} \tag{B1}$$

with

$$|\nu^+\rangle \equiv \lim_{\eta\to 0_+}\eta\int_{-\infty}^0 dt e^{\eta t}\mathcal{U}_w^\nu(0,t)|\nu\rangle. \tag{B2}$$

Here, $\mathcal{U}_w^\nu$ and U_w^ν are propagator and applied potential in the *interaction picture*

$$\mathcal{U}_w^\nu(t,0) = \mathcal{T}\exp\left\{-i\int_0^t dt' U_w^\nu(t')/\hbar\right\},$$

and

$$U_w^\nu(t) = \exp\{it\tilde{H}_\nu/\hbar\}(H-\tilde{H}_\nu)\exp\{-it\tilde{H}_\nu/\hbar\}.$$

For bound states of H_o, $|\nu\rangle = |b\rangle$, we set $\tilde{H}_\nu = H_o$, for scattering states of H_o, $|\nu\rangle = |\psi^+_{R,n,k}\rangle$, we choose $\tilde{H}_\nu = H_o + U_R(\infty)$.

Let $|\nu\rangle = |\psi^+_{R,n,k}\rangle$ be a scattering eigenstate of H_o with in asymptote $|\phi_{R,n,k}\rangle$ and $\tilde{H}_\nu = H_o + U_R(\infty)$. One may use the formal property of scattering states[68,37]

$$e^{-itH_o/\hbar}|\psi^+_{R,n,k}\rangle \to_{t\to-\infty} e^{-itH_{o,R}/\hbar}|\phi_{R,n,k}\rangle,$$

to rewrite (B2) as

$$\begin{aligned}|\nu^+\rangle &= \lim_{t\to-\infty} e^{itH/\hbar}e^{-it[H_o+U_R(\infty)]/\hbar}|\psi^+_{R,n,k}\rangle\\ &= \lim_{t\to-\infty} e^{itH/\hbar}e^{-it[H_{o,R}+U_R(\infty)]/\hbar}|\phi_{R,n,k}\rangle.\end{aligned}$$

But $H_{o,R}+U_R(\infty) = H_R$ is a reservoir Hamiltonian associated with H. Thus, $|\nu^+\rangle = |\Psi^+_{R,n,k}\rangle$, i.e., the scattering eigenstate of H with in asymptote $|\phi_{R,n,k}\rangle$. If $|\nu\rangle = |b\rangle$ is a bound state of H_o with eigenvalue E_b, one obtains

$$\begin{aligned}|b^+\rangle &= \lim_{\eta\to 0_+}\frac{i\eta\hbar}{E_b - H + i\eta\hbar}|b\rangle\\ &= |b\rangle + \lim_{\eta\to 0_+}(E_b - H + i\eta\hbar)^{-1}U|b\rangle.\end{aligned}$$

State $|b^+\rangle$ is that eigenstate $|B\rangle$ of H which, within first order of perturbation theory, is related to bound state $|b\rangle$ of H_o.

In summary, within linear response one obtains

$$\rho(0) = \sum_{R,n,k} f_{R,n,k}|\Psi^+_{R,n,k}\rangle\langle\Psi^+_{R,n,k}| + \sum_b f_b|B\rangle\langle B|, \tag{B3}$$

where $|\Psi^+_{R,n,k}\rangle$ and $|B\rangle$ denote the scattering and bound states of H. Thus, the steady-state density operator, within linear response, is closely related to the equilibrium density operator. The occupation probability of a bound state of H is that of the corresponding (via first-order perturbation theory) bound state $|b\rangle$ of H_o. Scattering states of H have the same occupation probability in $\rho(0)$ as scattering states of H_o with the same in asymptote (R,n,k) in ρ_o. This result is in agreement with the Kubo formula where the microbasis states are given a first-order correction in the perturbation U, while their occupation probability remains unaffected by the perturbation.[69] Moreover, when used for the calculation of the current density, (B3) leads to a conductance that is proportional to the transmission probability, establishing the equivalence between linear-response (Kubo) and conductance formula.

The linear-response expression (B3) will generally not be applicable to systems with finite applied bias. First, the eigenstates of H_o and $H = H_o + U$ will, in general, not be related to each other perturbatively. Therefore, adiabatic switching on of the perturbation U does not provide the correct ground or steady state of H. Second, even if H_o and H are related perturbatively to each other, higher-order terms in the applied bias may be required to quantitatively account for the current [see (A1)]. Finally, the small damping term which was formally introduced into the von Neumann equation to obtain $\rho(0)$ may not be appropriate. However, we shall argue that (B3) may provide a good approximation for finite applied bias, provided that reservoirs are properly defined.

Consider first a situation where neither H_o nor H have bound states, as is the case for our model of the Zener diode above. In this case, the limit $\eta \to 0$ may be split up into two separate limits, as in linear response. This is evident from the fact that scattering states incident through different reservoirs cannot be related to each other perturbatively. One obtains, for finite applied bias, a steady-state density operator

$$\rho(0) = \sum_{R,n,k} f_{R,n,k} |\Psi^+_{R,n,k}\rangle\langle\Psi^+_{R,n,k}|,$$

the same result as within linear response, where $f_{R,n,k}$ denotes the probability for occupancy of a scattering state with particle incidence from reservoir R and quantum numbers $\{n,k\}$. Note, however, that this corresponds to shifting the chemical potentials $\mu_R \to \mu_R + U_R(\infty)$ for incident-wave scattering states. The inadequacy of the coupling term to the bath, or equivalently, the adiabatic switch-on procedure is evidenced by the fact that, in general, application of a bias perturbs the asymptotic regions of the particle reservoirs which are supposed to be infinitely large. Again, this problem can be resolved only by assuming that the coupling between reservoirs with and without applied bias is infinitely small. Assuming finite coupling between the reservoirs and a finite perturbation is inconsistent with asymptotically unperturbed reservoirs in this coherent particle picture, we therefore may conclude that the linear-response expression of the steady-state density operator is valid for *finite* applied bias provided that the system with and without applied bias has no bound states and that the coupling between reservoirs is infinitesimally small.

A simple example is given in the form of a one-dimensional single (high) potential barrier. If the barrier is infinitely high, parallel shifting of the band edges to the left and to the right of the barrier will neither change scattering states nor their occupation probability, provided that the chemical potentials are shifted rigidly with the corresponding band edge. In the limit of sufficiently high, but finite barriers the linear-response result for $\rho(0)$ will provide a good approximation. Note that, for any one-dimensional system, (infinitesimally) small transmission coefficients are necessary to allow interpretation of the one-dimensional asymptotic regions as particle reservoirs and to make "bias across the barrier structure" a well-defined quantity.

Another frequently discussed example is a constriction which connects two two- (three-) dimensional reservoirs as sketched in Fig. 1.[64] In order for the steady-state current through the constriction to be finite, the average current density j deep inside of a reservoir must scale as d/L $[(d/L)^2]$. Here, d is the diameter of the constriction and L is the width of the reservoir before the thermodynamical limit is performed. Thus the transmission amplitude scales like $\sqrt{d/L}$ (d/L) and in the limit of infinite reservoirs goes to zero. A similar argument can be based on a comparison of the (local) density of states within the constriction and in the reservoirs.

In the presence of bound states for H_o the situation is different than in scattering theory where it is assumed that, in the distant past, the wave packet is a linear combination of eigenstates from the continuous spectrum of H_R and/or bound states of the full Hamiltonian H. However, the presence and occupancy of bound states of H_o has an influence of measure zero on the density operator $\rho(0)$ in the thermodynamic limit and is thus negligible for the computation of the current response. Consider, for instance a situation where H_o has a finite number of bound states $|b_i\rangle$ and H has none. Then turning on a bias at $t_o \to \infty$ will cause the bound state wave functions to spread to infinity such that, at $t = 0$, $\int_V dx |\langle x|b_i(0)\rangle|^2 = 0$ for any finite volume V. There is no contribution for local quantities, such as current and charge density. If, on the other hand, H_o has no bound states but H does, adiabatic switching on of the perturbation does not lead to a population of the bound states at time t=0 and the procedure fails to give the new ground or stationary state. This is a well-known result in connection with the Gell-Mann-Low theorem and is closely related to the fact that Møller operators are isometric rather than unitary when the system supports bound states.[67,37]

Thus we are led to the conclusion that, for all practical purposes in which the *scattering states are defined with respect to the particle reservoirs, and H has no bound states, and where an independent-particle picture provides a good approximation*, (B3) may be used to calculate the current response of a mesoscopic system for *finite* applied bias. This form of $\rho(0)$, as well as the definition of "applied bias," becomes phenomenological if, for finite bias, proper reservoirs, as defined above, are not incorporated into the calculation of scattering states (and/or transmission amplitudes).

APPENDIX C: ORTHOGONALITY OF SCATTERING STATES

Orthonormality and, together with bound states, completeness of (single-particle) scattering states for situations encountered in mesoscopic systems of the kind specified above (and the Zener diode, in particular,) can be shown by applying concepts from time-dependent scattering theory, provided condition (5) is met.[37,65,68,70,71]

Let us consider two different wave packets each of which characterizes a particle incident through some reservoir $R(R')$ and using the notation introduced in Sec. II. For $t \to -\infty$, the particles are arbitrarily far away inside reservoir $R(R')$ and the two wave packets may be written[68]

$$|\bar{\phi}^{(1)}_R(t)\rangle = \sum_n \int dk\, C^{(1)}_R(n,k) |\phi_{R,n,k}\rangle \times \exp\{-iE_{R,n}(k)t/\hbar\}, \tag{C1}$$

and

$$|\bar{\phi}^{(2)}_{R'}(t)\rangle = \sum_{n'} \int dk\, C^{(2)}_{R'}(n',k) |\phi_{R',n',k}\rangle \times \exp\{-iE_{R',n'}(k)t/\hbar\}. \tag{C2}$$

Within the same reservoir, normalized channel states $|\phi_{R,n,k}\rangle$, which are eigenstates of H_R with eigenvalue $E_{R,n}(k)$, are mutually orthogonal. Channel states associated with different reservoirs need not be orthogonal to each other. These wave packets move freely in reservoir $R(R')$ in the remote past and, as a more detailed investigation shows, develop into the wave functions[68]

$$|\bar{\Psi}_R^{(1)}(t)\rangle = \sum_n \int dk\, C_R^{(1)}(n,k)|\Psi_{R,n}^+(k)\rangle \times \exp\{-iE_{R,n}(k)t/\hbar\}, \quad \text{(C3)}$$

and

$$|\bar{\Psi}_{R'}^{(2)}(t)\rangle = \sum_{n'} \int dk\, C_{R'}^{(2)}(n',k)|\Psi_{R',n',k}^+\rangle \times \exp\{-iE_{R',n'}(k)t/\hbar\}, \quad \text{(C4)}$$

respectively, at finite time t. $|\Psi_{R,n,k}^+\rangle$ are scattering eigenstates of H.

First consider $R = R'$. Using (C1), (C2), and (C3), and the orthonormality of channel states $|\phi_{R,n,k}\rangle$ for given R, one finds

$$\begin{aligned}\langle\bar{\Psi}_R^{(1)}(0)|\bar{\Psi}_R^{(2)}(0)\rangle &= \langle\bar{\Psi}_R^{(1)}(t)|\bar{\Psi}_R^{(2)}(t)\rangle \\ &\overset{t\to-\infty}{\to} \langle\bar{\phi}_R^{(1)}(t)|\bar{\phi}_R^{(2)}(t)\rangle \\ &= \int dk \sum_n C_R^{(1)}(n,k)^* \\ &\quad \times C_R^{(2)}(n,k).\end{aligned}$$

As the expansion coefficients $C_R^{(i)}(n,k)$ are arbitrary, one is led to

$$\langle\Psi_{R,n,k}^+|\Psi_{R,n',k'}^+\rangle = \delta_{n,n'}\delta_{k,k'}.$$

Thus scattering states associated with the same reservoir are mutually orthonormal.

Next consider two wave packets that characterize a particle incident through reservoir R and R', $R \neq R'$, respectively. For $t \to -\infty$, the two particles propagate infinitely far inside their respective reservoirs. Owing to this spatial separation the overlap between the two wave packets is zero. The two wave packets evolve into (C3) and (C4). Thus

$$\begin{aligned}\langle\bar{\Psi}_R^{(1)}(0)|\bar{\Psi}_{R'}^{(2)}(0)\rangle &= \langle\bar{\Psi}_R^{(1)}(t)|\bar{\Psi}_{R'}^{(2)}(t)\rangle \\ &\overset{t\to-\infty}{\to} \langle\bar{\phi}_R^{(1)}(t)|\bar{\phi}_{R'}^{(2)}(t)\rangle = 0, \text{ for } R \neq R'.\end{aligned}$$

Again, expansion coefficients are arbitrary and one concludes

$$\langle\Psi_{R,n,k}^+|\Psi_{R',n',k'}^+\rangle = 0, \text{ for } R \neq R'.$$

Note that channel states belonging to different reservoirs need not be orthogonal to each other. Consider, for instance, carrier scattering at a heterointerface between two crystals. The channel states are Bloch states and there is no reason why Bloch states belonging to two different crystals should be orthogonal to each other. Yet, associated scattering states are mutually orthogonal. Similarly, orthogonality of scattering states $\{|\Psi_{R,n,k}^-\rangle\}$ can be shown. Of course, scattering states $\{|\Psi_{R,n,k}^+\rangle\}$ and $\{|\Psi_{R,n,k}^-\rangle\}$ are not orthogonal to each other. In a similar fashion one may show orthogonality between scattering states and bound states. For the proof of completeness of bound states and scattering states we refer to Ref. 68. This proof is rather general. It applies to any system which supports only bound states and scattering states and for which (5) holds.

APPENDIX D: THE S MATRIX FOR MESOSCOPIC SYSTEMS

In this section we show that the S matrix defined in (10) is unitarity, which is intimately linked to orthonormality of scattering states. In what follows, we consider a system as described in Sec. II and allow an arbitrary number of reservoirs with different characteristics, such as electronic structure and reservoir dimensions D_R.

Unitarity of S may be shown by considering wave packets,

$$|\bar{\Psi}_{R,n}(t)\rangle = \int d^{(D_R)}k C_{R,n,k}|\Psi_{R,n,k}^+(t)\rangle,$$

incident through channels (R,n).

Equating $\langle\bar{\Psi}_{R,n}(t)|\bar{\Psi}_{R',n'}(t)\rangle$ for time $t \to -\infty$ and $t \to +\infty$ gives, [see Eq. (10)],

$$\begin{aligned}&\delta_{R,R'}\delta_{n,n'}\int d^{(D_R)}k|C_{R,n,k^+}|^2 \\ &= \sum_{\bar{R},\bar{n}}\int dk \int_{E_{R,n}(k)} \frac{d\mathcal{S}_{R',n'}}{|\nabla E_{R',n'}(k')|}\int_{E_{R,n}(k)} d\mathcal{S}_{\bar{R},\bar{n}} \\ &\quad \times b^*_{(R,n,k^-\to\bar{R},\bar{n},\bar{k}^+)} b_{(R',n',k'^-\to\bar{R},\bar{n},\bar{k}^+)} \\ &\quad \times |\nabla E_{\bar{R},\bar{n}}(\bar{k})| C^*_{R,n,k^+} C_{R',n',k'^+}. \quad \text{(D1)}\end{aligned}$$

Validity of this expression for arbitrary expansion coefficients $C_{R,n,k}$ demonstrates unitarity of the S matrix. In particular, Kirchhoff's junction rule (conservation of charge) applied to scattering state $\Psi_{R,n,k}^+$ gives

$$\sum_{\bar{R},\bar{n}}\int_{E_{R,n}(k)} d\mathcal{S}_{\bar{R},\bar{n}}|b_{(R,n,k^-\to\bar{R},\bar{n},\bar{k}^+)}|^2 \frac{|\nabla E_{\bar{R},\bar{n}}(\bar{k})|}{|\nabla E_{R,n}(k)|} = 1.$$

This identity is a general version of $T + R = 1$ for one-dimensional systems and expresses that a scattering state is a stationary state of the system whose probability current density into the system balances the probability current density out of the system. Time-reversal symmetry leads to additional relations among S matrix elements.[72]

[1] C. B. Duke, in *Solid State Physics*, edited by F. Seitz and D. Turnbull (Academic Press, New York, 1969), Suppl. 10.
[2] D. K. Roy, *Quantum Mechanical Tunneling and its Applications* (World Scientific, Singapore, 1986).
[3] D. Emin and C. F. Hart, Phys. Rev. B **36**, 7353 (1987); **41**, 3859 (1990); **43**, 2426 (1991); **43**, 4521 (1991).
[4] L. Kleinman, Phys. Rev. B **41**, 3857 (1990).
[5] D. A. Page and E. Brown, Phys. Rev. B **43**, 2423 (1991).
[6] J. Zak, Phys. Rev. B **43**, 4519 (1991).
[7] G. H. Wannier, Phys. Rev. **100**, 1227 (1955); **101**, 1835 (1956); **117**, 432 (1960); Rev. Mod. Phys. **34**, 645 (1962).
[8] J. Zak, Phys. Rev. Lett. **20**, 1477 (1968); Phys. Rev. **181**, 1366 (1969).
[9] J. B. Krieger and G. J. Iafrate, Phys. Rev. B **33**, 5494 (1986).
[10] G. Nenciu, Rev. Mod. Phys. **63**, 91 (1991).
[11] J. E. Avron, J. Zak, A. Grossmann, and L. Gunther, J. Math. Phys. **18**, 918 (1977).
[12] I. W. Herbst and J. S. Howland, Commun. Math. Phys. **80**, 23 (1981).
[13] F. Bentosela and V. Grecchi, Commun. Math. Phys. **142**, 169 (1991).
[14] Andrea Sacchetti, Helv. Phys. Acta **65**, 11 (1992).
[15] T. Nakanishi, T. Ohtsuki, and M. Saitoh, in *21st International Conference on the Physics of Semiconductors, Beijing, 1992*, edited by P. Jiang and H.-Z. Zheng (World Scientific, Singapore, 1992), Vol. 1, p. 741.
[16] A. G. Chynoweth, G. H. Wannier, R. A. Logan, and D. E. Thomas, Phys. Rev. Lett. **5**, 57 (1960).
[17] S. Maekawa, Phys. Rev. Lett. **24**, 1174 (1970).
[18] R. W. Koss and L. M. Lambert, Phys. Rev. B **5**, 1479 (1972).
[19] D. May and A. Vecht, J. Phys. C **8**, L505 (1975).
[20] E. E. Mendez, F. Agulló-Rueda, and J. M. Hong, Phys. Rev. Lett. **60**, 2426 (1988).
[21] C. Waschke, H. G. Roskos, R. Schwedler, K. Leo, H. Kurz, and K. Köhler, Phys. Rev. Lett. **70**, 3319 (1993).
[22] M. Yamaguchi, M. Morifuji, H. Kubo, K. Taniguchi, C. Hamaguchi, C. Gmachl, and E. Gornik, Solid-State Electron. **37**, 839 (1994).
[23] E. O. Kane, J. Phys. Chem. Solids **12**, 181 (1959).
[24] E. O. Kane, J. Appl. Phys. **32**, 83 (1961).
[25] E. I. Blount, in *Solid State Physics*, edited by F. Seitz and D. Turnbull (Academic Press, New York, 1962), Vol. 13.
[26] P. N. Argyres, Phys. Rev. **126**, 1386 (1962).
[27] J. Callaway, *Quantum Theory of the Solid State* (Academic Press, San Diego, 1991).
[28] Ping Ao and J. Rammer, Phys. Rev. B **44**, 11 494 (1991).
[29] P. N. Argyres and S. Sfiat, J. Phys. Condens. Matter **2**, 7089 (1990).
[30] R. Landauer, IBM J. Res. Dev. **32**, 306 (1988).
[31] M. Büttiker, IBM J. Res. Dev. **32**, 317 (1988).
[32] D. D. Coon and H. C. Liu, Appl. Phys. Lett. **47**, 172 (1985).
[33] A. D. Stone and A. Szafer, IBM J. Res. Dev. **32**, 384 (1988).
[34] A. M. Kriman, N. C. Kluksdahl, and D. K. Ferry, Phys. Rev. B **36**, 5953 (1987); A. M. Kriman, A. Szafer, A. D. Stone, and D. K. Ferry (unpublished).
[35] E. B. Davies and B. Simon, Commun. Math. Phys. **63**, 277 (1978).
[36] J. U. Nöckel, A. D. Stone, and H. U. Baranger, Phys. Rev. B **48**, 17 569 (1993), and references therein.
[37] J. R. Taylor, *Scattering Theory* (Wiley, New York, 1972).
[38] W. Pötz (unpublished).
[39] D. N. Zubarev, *Nonequilibrium Statistical Thermodynamics* (Plenum, New York, 1974).
[40] W. Pötz and J. Zhang, Phys. Rev. B **45**, 11 496 (1992).
[41] G. C. Osbourn and D. L. Smith, Phys. Rev. B **19**, 2124 (1979).
[42] J. N. Schulman and Yia-Chung Chang, Phys. Rev. B **27**, 2346 (1983).
[43] D. Z.-Y. Ting, E. T. Yu, and T. C. McGill, Phys. Rev. B **45**, 3583 (1992).
[44] P. Vogl, H. P. Hjalmarson, and J. D. Dow, J. Phys. Chem. Solids **44**, 365 (1983).
[45] J. N. Schulman and Yia-Chung Chang, Phys. Rev. B **31**, 2056 (1985).
[46] For a linear potential profile and localized basis states that are angular momentum eigenfunctions, the shown approximate equality holds exactly, apart from an intra-atomic Stark effect which is negligible for realistic applied fields.
[47] S. M. Sze, *Physics of Semiconductor Devices* (Wiley, New York, 1981).
[48] T. B. Boykin, J. P. A. van der Wagt, and J. S. Harris, Jr., Phys. Rev. B **43**, 4777 (1991).
[49] J. N. Schulman and D. Z.-Y. Ting, Phys. Rev. B **45**, 6282 (1992).
[50] S. Froyen, Phys. Rev. B **39**, 3168 (1989).
[51] Empirical pseudopotential calculations for bulk GaAs [J. R. Chelikowsky and M. L. Cohen, Phys. Rev. B **14**, 556 (1976)] predict a width of the first conduction band along the [001] direction of $\Delta_{c1} = 1.9$ eV. We note that along the [111] direction, this width is smaller and given by $\Delta_{c1} = 1.0$ eV.
[52] A. M. Berezhkovskii and A. A. Ovchinnikov, Fiz. Tverd. Tela (Leningrad) **18**, 3273 (1976) [Sov. Phys. Solid State **18**, 1908 (1976)].
[53] L. V. Keldysh, Zh. Eksp. Teor. Fiz. **33**, 59 (1958) [Sov. Phys. JETP **6**, 763 (1958)]; **34**, 101 (1958) [**7**, 665 (1958)].
[54] M. Claassen (private communication).
[55] D. J. Dumin and G. L. Pearson, J. Appl. Phys. **36**, 3418 (1965).
[56] L. Gaul, S. Huber, J. Freyer, and M. Claassen, Solid-State Electron. **34**, 723 (1991); D. Liebig, P. Lugli, P. Vogl, M. Claassen, and W. Harth, Microelectron. Eng. **19**, 127 (1992).
[57] J. B. Krieger, Ann. Phys. **36**, 1 (1966).
[58] A. M. Berezhkovskii and A. A. Ovchinnikov, Phys. Status Solidi B **117**, 289 (1983).
[59] P. J. Price and J. M. Radcliffe, IBM J. Res. Dev. **3**, 364 (1959).
[60] R. Enderlein and K. Peuker, Phys. Status Solidi B **48**, 231 (1971).
[61] A. Schenk, Solid-State Electron. **36**, 19 (1992).
[62] See, for example, M. L. Leadbeater, E. S. Alves, L. Eaves, M. Henini, O. H. Hughes, A. Celeste, J. C. Portal, G. Hill, and M. A. Pate, Phys. Rev. B **39**, 3438 (1989).
[63] W. Pötz and Z. Q. Li, Solid-State Electron. **32**, 1353 (1989).
[64] I. B. Levinson, Zh. Eksp. Teor. Fiz. **95**, 2175 (1989) [Sov. Phys. JETP **68**, 1257 (1989)].
[65] M. L. Goldberger and K. M. Watson, *Collision Theory* (Wiley, New York, 1964).
[66] Note a subtle point. Really, H needs to be found via a time-dependent study of the problem including interaction mechanisms which ensure existence of such a steady state. In this construction, one makes assumptions upon the form of self-consistent Hamiltonian H but one does not discuss the dynamics of how this state has been established.

[67] M. Gell-Mann and F. Low, Phys. Rev. **84**, 350 (1951).
[68] J. E. G. Farina, in *International Encyclopedia of Physical Chemistry and Chemical Physics*, edited by R. McWeeny (Pergamon, Oxford, 1975), Topic 2, Vol. 1.
[69] E. Fick and G. Sauermann, *The Quantum Statistics of Dynamic Processes* (Springer, Berlin, 1990).
[70] R. G. Newton, *Scattering Theory of Waves and Particles* (McGraw-Hill, New York, 1966).
[71] C. J. Joachain, *Quantum Collision Theory* (North-Holland, Amsterdam, 1983).
[72] D. C. Langreth and E. Abrahams, Phys. Rev. B **24**, 2978 (1981).